

SKB

**TECHNICAL
REPORT**

90-22

Near-field high-temperature transport: Evidence from the genesis of the Osamu Utsumi uranium mine, Poços de Caldas alkaline complex, Brazil

L. M. Cathles¹, M. E. Shea²

¹ Cornell University, Department of Geological Sciences

² University of Chicago, Department of Geological Sciences

1990

SVENSK KÄRNBRÄNSLEHANTERING AB

SWEDISH NUCLEAR FUEL AND WASTE MANAGEMENT CO

BOX 5864 S-102 48 STOCKHOLM

TEL 08-665 28 00 TELEX 13108 SKB S

TELEFAX 08-661 57 19



NAGRA **NTB 90 - 31**
SKB **TR 90 - 22**
UK DOE **WR 90 - 053**

Poços de Caldas Report No. 13

**Near-field high-temperature
transport: Evidence from the
genesis of the Osamu Utsumi
uranium mine, Poços de Caldas
alkaline complex, Brazil**

An international project with the participation of Brazil, Sweden (SKB), Switzerland (NAGRA), United Kingdom (UK DOE) and USA (US DOE). The project is managed by SKB, Swedish Nuclear Fuel and Waste Management Co.

NEAR-FIELD HIGH-TEMPERATURE TRANSPORT: EVIDENCE
FROM THE GENESIS OF THE OSAMU UTSUMI URANIUM MINE,
POÇOS DE CALDAS ALKALINE COMPLEX, BRAZIL

L. M. Cathles¹
M. E. Shea²

¹Cornell University, Department of Geological
Sciences

²University of Chicago, Department of Geophysical
Sciences

1990

This report concerns a study which was conducted for SKB. The conclusions and viewpoints presented in the report are those of the author(s) and do not necessarily coincide with those of the client.

Information on SKB technical reports from 1977-1978 (TR 121), 1979 (TR 79-28), 1980 (TR 80-26), 1981 (TR 81-17), 1982 (TR 82-28), 1983 (TR 83-77), 1984 (TR 85-01), 1985 (TR 85-20), 1986 (TR 86-31), 1987 (TR 87-33), 1988 (TR 88-32) and 1989 (TR 89-40) is available through SKB.

Near-field high-temperature transport: Evidence from the genesis of the Osamu Utsumi uranium mine, Poços de Caldas alkaline complex, Brazil.

L.M. CATHLES¹ and M.E. SHEA²

¹Cornell University, Department of Geological Sciences, Ithaca, New York, (USA).

²University of Chicago, Department of Geophysical Sciences, 5734, S. Ellis Avenue, Chicago, Illinois (USA).

Abstract

The chemical, isotopic and mineralogical alteration which occurred during primary uranium ore deposition at the breccia pipe-hosted Osamu Utsumi mine, Poços de Caldas, Brazil, was studied as a natural analogue for near-field radionuclide migration. Chemical and isotopic alteration models were combined with finite difference models of the convective cooling of caldera intrusives. The modelling indicates that the intense chemical, isotopic and mineralogical alteration of the Osamu Utsumi breccia pipe requires the circulation of $>10^5$ kg of boiling hydrothermal fluid $>220^\circ\text{C}$ through each square centimeter cross-section of the pipe. The circulation can be driven by heat from a 6 km diameter intrusion extending to 10 km depth. Even with this large amount of circulation concentrated in the permeable breccia pipe, uranium solubilities must be 2 1/2 orders of magnitude greater than indicated in the most recent experiments (and more in line with previous estimates) to produce the primary uranium mineralization at the Osamu Utsumi mine.

The same models applied to a hypothetical high-temperature waste repository show that heat from radioactive decay will produce a hydrothermal circulation system remarkably similar to that studied at the natural analogue site at Poços de Caldas. The depth of fluid convection induced by the hypothetical repository would be 5 to 10 km, the maximum temperature $\sim 300^\circ\text{C}$, the lifetime of the high-temperature phase a few 1000s of years and boiling would cause most of the alteration of the waste repository. The physical analysis emphasizes the importance of permeability on a 10 x 10 x 10 km scale in controlling the potential amount of circulation through the hypothetical repository.

Application of the chemical models successfully used to interpret mineralization and alteration at the Osamu Utsumi mine to the hypothetical waste repository shows that, even in a worst case scenario (waste emplaced in a permeable host rock with no measures taken to inhibit flow through the repository), the amount of hydrothermal alteration in the hypothetical repository will be $\sim 0.1\%$ of that in the breccia pipe at the Osamu Utsumi

mine. Assuming no barriers to uranium mobility, uranium precipitation above the hypothetical repository would be 0.05 ppm (rather than 50 ppm), hydrothermal alteration 0.03 wt.% (rather than 30 wt.%), etc.

The analysis indicates that mineralogical alteration is extremely sensitive to thermodynamic data. Prediction of mineralogical alteration (which may be necessary to predict the migration of radionuclides other than uranium, for example) probably cannot be based directly on even very carefully collected laboratory thermodynamic data. Mineralogical complexities of the system, as well as database uncertainties, will require calibration of the thermodynamic framework against mineralogical alteration observed in the laboratory or field by procedures briefly described.

Zusammenfassung

Die chemischen, isotopischen und mineralogischen Veränderungen, die während der primären Uranerzablagerung in der Schlotbrekzie angelegten Osamu Utsumi Mine in Poços de Caldas, Brasilien, auftraten, wurden als natürliches Analogon zur Nahfeld-Radionuklidmigration studiert. Chemische und isotopische Veränderungsmodelle wurden mit finiten Differenzmodellen des konvektiven Abkühlens der Caldera Intrusion kombiniert. Die Resultate der Modelle deuten darauf hin, dass diese intensiven chemischen, isotopischen und mineralogischen Veränderungen der Schlotbrekzie einer Zirkulation von $>10^5$ kg kochender hydrothermaler Flüssigkeit $>220^\circ\text{C}$ durch jeden Quadrat-zentimeter Querschnitt des Schlotes bedarf. Die Zirkulation kann durch die Hitze einer Intrusion von 6 km Durchmesser und einer Tiefe von 10 km unterhalten werden. Selbst mit dieser enormen Zirkulationsmenge, die in der permeablen Schlotbrekzie konzentriert ist, müsste die Uranlöslichkeit nur 2 1/2 Grössenordnungen mal grösser sein, als aufgrund der neuesten Experimente (und näher zu früheren Schätzungen) angenommen wurde, um die primäre Uranmineralisation in der Osamu Utsumi Mine zu erzeugen.

Die gleichen Modelle, angewandt auf ein hypothetisches Hochtemperatur-Endlager zeigen, dass die durch radioaktiven Zerfall hervorgerufene Hitze, ein hydrothermales Zirkulationssystem erzeugt, das erstaunliche Ähnlichkeiten mit dem der Analog-Untersuchungsstelle von Poços de Caldas aufweist. Die Tiefe der Flüssigkeitskonvektion, die durch das hypothetische Endlager ausgelöst würde, läge bei 5 bis 10 km, die maximale Temperatur bei $\sim 300^\circ\text{C}$, die Zeitspanne der Hochtemperaturphase würde sich über einige tausende von Jahren erstrecken, und das Kochen würde die meisten Veränderungen des Endlagers verursachen. Die physikalische Analyse hebt die Wichtigkeit der Permabilität einer Zone der Grössenordnung von $10 \times 10 \times 10$ km hervor, um den potentiellen Umfang der Zirkulation durch das hypothetische Endlager zu ermöglichen.

Die Anwendung des chemischen Modells, das erfolgreich zur Interpretation der Mineralisation und der Veränderungen in der Osamu Utsumi Mine eingesetzt wurde, auf das hypothetische Endlager zeigt, dass selbst beim Eintreffen des schlimmsten Falles (Abfall plaziert in permeablem Wirtgestein, ohne Massnahmen den Fluss durch das Lager zu verhindern) der Umfang der hydrothermalen Veränderungen im hypothetischen Endlager $\sim 0.1\%$ der Veränderung der Schlotbrekzie in der Osamu Utsumi Mine entsprechen würde. Unter der Annahme, dass keine Barrieren gegen die Uranmobilität beständen, würde die Uranausfällung über dem hypothetischen Endlager 0.05 ppm (anstatt 50 ppm) betragen, die hydrothermale Veränderung 0,03 Gew.% (anstatt 30 Gew.%) ausmachen, usw.

Die Analyse zeigt, dass mineralogische Veränderungen extrem empfindlich auf thermodynamische Daten reagieren. Vorhersagen über mineralogische Veränderungen (die nötig sein könnten, zum Beispiel zur Vorhersage der Migration von Radionukliden anderer Art als Uran) können wahrscheinlich nicht direkt auf noch so vorsichtig gesammelte thermodynamische Laborresultate basiert werden. Die mineralogische Komplexität des Systems sowie die Unsicherheit gewisser Daten, bedingen die Anpassung der thermodynamischen Grundstrukturen an die mineralogischen Veränderungen, wie sie im Labor oder im Feld durch die kurz beschriebenen Vorgänge beobachtet werden.

Résumé

Les altérations chimiques, isotopiques et minéralogiques qui se sont produites lors du dépôt primaire de minerais d'uranium dans la brèche de cheminée de la mine d'Osamu Utsumi, à Poços de Caldas au Brésil, ont été étudiées à titre d'analogies naturelles pour la migration de radionucléides dans le champ proche. Des modèles d'altérations chimiques et isotopiques ont été combinés avec des modèles à différences finies du refroidissement par convection des intrusions dans la caldera. La modélisation montre que l'intense altération chimique, isotopique et minérale de la cheminée d'Osamu Utsumi nécessiterait la circulation de $>10^5$ kg de fluide hydrothermal bouillant à $>220^\circ\text{C}$ au travers de chaque cm carré de section de cheminée. Cette circulation pourrait être engendrée par la chaleur provenant d'une intrusion de 6 km de diamètre s'étendant à une profondeur de 10 km. Même avec une telle circulation, concentrée dans la cheminée perméable, les solubilités d'uranium devraient être supérieures de 2 1/2 ordres de grandeur par rapport à celles indiquées par les expériences les plus récentes (et plus en concordance avec les estimations précédentes) pour engendrer la minéralisation primaire d'uranium dans la mine d'Osamu Utsumi.

Les mêmes modèles appliqués à un dépôt de déchets radioactifs hypothétique à haute température montre que la chaleur provenant de la désintégration des déchets engendrerait un système de circulation hydrothermale remarquablement similaire à celui étudié sur le site d'analogies naturelles de Poços de Caldas. La profondeur de la convection de fluide engendrée par le dépôt hypothétique serait de 5 à 10 km, la température maximum d'env. 300°C , la durée de la phase à haute température de quelques milliers d'années et l'ébullition provoquerait la plus grande partie des altérations du dépôt de déchets radioactifs. L'analyse physique met en évidence l'importance de la perméabilité sur une échelle de $10 \times 10 \times 10$ km pour le contrôle du degré de circulation potentielle à travers le dépôt hypothétique.

L'application des modèles chimiques au dépôt de déchets hypothétique, utilisés avec succès pour interpréter les minéralisations et altérations de la mine d'Osamu Utsumi, montre que, même dans le cas d'un scénario catastrophe (déchets placés dans une roche d'accueil perméable en l'absence de mesures limitant la circulation à travers le dépôt) le degré d'altération hydrothermale dans le dépôt hypothétique ne serait que d'env. 0.1% de celui de la cheminée de la mine d'Osamu Utsumi. Dans l'hypothèse d'absence de frein à la mobilité de l'uranium, la précipitation d'uranium au-dessus du dépôt hypothétique serait de 0.05 ppm (plutôt que de 50 ppm), l'altération hydrothermale de 0.03 % poids (au lieu de 30% poids), etc.

L'analyse montre que les altérations minéralogiques sont très sensibles aux paramètres thermodynamiques. La prédiction d'altérations minéralogiques (qui, par exemple, pourrait être nécessaire pour pronostiquer la migration de radionucléides autres que l'uranium) n'est probablement pas possible en s'appuyant sur les données thermodynamiques de laboratoire, même si le processus de détermination est très soigneux. Les complexités minéralogiques du système, de même que les incertitudes dans la banque de données, nécessiteront la calibration du cadre thermodynamique par rapport aux altérations minéralogiques observées en laboratoire ou sur le terrain selon des procédures brièvement décrites.

Preface

The Poços de Caldas Project was designed to study processes occurring in a natural environment which contains many features of relevance for the safety assessment of radioactive waste disposal. The study area, in the State of Minas Gerais, Brazil, is a region of high natural radioactivity associated with volcanic rocks, geothermal springs and uranium ore deposits. It contains two sites of particular interest on which the project work was focussed: the Osamu Utsumi uranium mine and the Morro do Ferro thorium/rare-earth ore body. The first site is notable in particular for the prominent redox fronts contained in the rock, while Morro do Ferro was already well-known as one of the most naturally radioactive locations on the surface of the Earth, owing to the high thorium ore grade and the shallow, localised nature of the deposit.

The features displayed by these two sites presented the opportunity to study a number of issues of concern in repository performance assessment. The four objectives set after the first-year feasibility study were:

1. Testing of equilibrium thermodynamic codes and their associated databases used to evaluate rock/water interactions and solubility/speciation of elements.
2. Determining interactions of natural groundwater colloids with radionuclides and mineral surfaces, with emphasis on their role in radionuclide transport processes.
3. Producing a model of the evolution and movement of redox fronts, with the additional aim of understanding long-term, large-scale movements of trace elements and rare-earths over the front (including, if possible, natural Pu and Tc).
4. Modelling migration of rare-earths (REE) and U-Th series radionuclides during hydrothermal activity similar to that anticipated in the very near-field of some spent-fuel repositories.

The project ran for three and a half years from June 1986 until December 1989 under the joint sponsorship of SKB (Sweden), NAGRA (Switzerland), the Department of the Environment (UK) and the Department of Energy (USA), with considerable support from a number of organisations in Brazil, notably Nuclebrás (now Urânio do Brasil). The first-year feasibility study was followed by two and a half years of data collection and interpretation, focussed on the four objectives above.

This report is one of a series of 15, summarising the technical aspects of the work and presenting the background data. A complete list of reports is given below. Those in series A present data and interpretations of the sites, while those in series B present the results of modelling the data with performance assessment objectives in mind. The main findings of the project are presented in a separate summary (no. 15).

The work presented in this report represents an attempt to model the rock alteration and migration of radionuclides during hydrothermal activity, similar to that anticipated in the very near-field of some spent fuel repositories (i.e. the fourth objective of the project).

Poços de Caldas Project Report Series

Series A: Data, Descriptive, Interpretation

Report No.	Topic	Authors (Lead in Capitals)
1.	The regional geology, mineralogy and geochemistry of the Poços de Caldas alkaline caldera complex, Minas Gerais, Brazil.	SCHORSCHER, Shea.
2.	Mineralogy, petrology and geochemistry of the Poços de Caldas analogue study sites, Minas Gerais, Brazil. I: Osamu Utsumi uranium mine.	WABER, Schorscher, Peters.
3.	Mineralogy, petrology and geochemistry of the Poços de Caldas analogue study sites, Minas Gerais, Brazil. II: Morro do Ferro.	WABER.
4.	Isotopic geochemical characterization of selected nepheline syenites and phonolites from the Poços de Caldas alkaline complex, Minas Gerais, Brazil.	SHEA.
5.	Geomorphological and hydrogeological features of the Poços de Caldas caldera and the Osamu Utsumi mine and Morro do Ferro analogue study sites, Brazil.	HOLMES, Pitty, Noy.
6.	Chemical and isotopic composition of groundwaters and their seasonal variability at the Osamu Utsumi and Morro do Ferro analogue study sites, Poços de Caldas, Brazil.	NORDSTROM, Smellie, Wolf.
7.	Natural radionuclide and stable element studies of rock samples from the Osamu Utsumi mine and Morro do Ferro analogue study sites, Poços de Caldas, Brazil.	MacKENZIE, Scott, Linsalata, Miekeley, Osmond, Curtis.
8.	Natural series radionuclide and rare-earth element geochemistry of waters from the Osamu Utsumi mine and Morro do Ferro analogue study sites, Poços de Caldas, Brazil.	MIEKELEY, Coutinho de Jesus, Porto da Silveira, Linsalata, Morse, Osmond.

Report No.	Topic	Authors (Lead in Capitals)
9.	Chemical and physical characterisation of suspended particles and colloids in waters from the Osamu Utsumi mine and Morro do Ferro analogue study sites, Poços de Caldas, Brazil.	MIEKELEY, Coutinho de Jesus, Porto da Silveira, Degueldre.
10.	Microbiological analysis at the Osamu Utsumi mine and Morro do Ferro analogue study sites, Poços de Caldas, Brazil.	WEST, Vialta, McKinley.

Series B: Predictive Modelling and Performance Assessment

11.	Testing of geochemical models in the Poços de Caldas analogue study.	BRUNO, Cross, Eikenberg, McKinley, Read, Sandino, Sellin.
12.	Testing models of redox front migration and geochemistry at the Osamu Utsumi mine and Morro do Ferro analogue study sites, Poços de Caldas, Brazil.	Ed: McKINLEY, Cross, Haworth, Lichtner, MacKenzie, Moreno, Neretnieks, Nordstrom, Read, Romero, Scott, Sharland, Tweed.
13.	Near-field high-temperature transport: Evidence from the genesis of the Osamu Utsumi uranium mine, Poços de Caldas alkaline complex, Brazil.	CATHLES, Shea.
14.	Geochemical modelling of water-rock interactions at the Osamu Utsumi mine and Morro do Ferro analogue study sites, Poços de Caldas, Brazil.	NORDSTROM, Puigdomènech, McNutt.

Summary Report

15.	The Poços de Caldas Project: Summary and implications for radioactive waste management.	CHAPMAN, McKinley, Shea, Smellie.
-----	---	-----------------------------------

Contents

	page
Abstract	vii
Preface	vii
1. Introduction	1
2. Uranium mineralization at the Osamu Utsumi mine	3
2.1. The physical system	3
2.2. Chemical changes	7
2.3. Petrologic changes	9
2.4. Other observations	13
3. Calculation of the fluid circulation responsible for uranium mineralization and alteration at the Osamu Utsumi mine	14
3.1. Base physical model of fluid circulation	14
3.2. Circulation required for the low-grade hydrothermal uranium mineralization	19
3.3. Circulation required for isotopic alteration	21
3.4. Circulation required for chemical alteration	23
3.4.1. Silica transport	25
3.4.2. Potassium, aluminium and sodium transport	25
3.5. Increasing hydrothermal circulation through the breccia at the Osamu Utsumi mine	32
3.6. A circulation model compatible with all chemical data	34
4. Chemical experiments to test alteration models	35
5. Prediction of the near-field uranium transport and alteration at a hypothetical high-level waste repository	37
6. Conclusions and recommendations for future work	42
7. References	43

1. Introduction

Uranium in the Poços de Caldas alkaline complex was precipitated from circulating hydrothermal fluids. The fluids were driven by heat introduced by an episode of syenitic ring dyke injection and magma intrusion that caused resurgent doming of the Poços de Caldas caldera 76 million years ago (Schorscher and Shea; Shea, this report series; Repts. 1 and 4). This “primary” uranium was subsequently remobilized and concentrated to ore grade by weathering and groundwater infiltration. The low-temperature remobilization by weathering and groundwater flow, which has continued to nearly the present time, provides a natural analogue for certain aspects of the far-field migration of radionuclides and was the main focus of the Poços de Caldas project. The much higher-temperature processes that led to the primary concentration of uranium are a natural analogue for certain aspects of the near-field rock alteration and radionuclide migration and were the subject of the modelling studies reported here.

Both the hydrothermal alteration and the primary mineralization are related to the volume of hydrothermal fluid circulation. Models that constrain the amount of fluid flow that can be produced by intrusions of reasonable size can therefore help to define the nature of primary mineralization and alteration.

The Poços de Caldas observations indicate how rock may be altered over relatively protracted periods of time ($10^3 - 10^4$ a) by high-temperature fluid circulation and how alteration is related to uranium transport. The models developed allow these observations to be applied to rock alteration in the near-field of hypothetical high-level waste repositories. The flexibility of the procedures developed would also allow different rock types to be considered. In what follows, the primary mineralization and alteration at the Osamu Utsumi mine is first briefly summarized. The steps taken to model this primary alteration and mineralization and to test the models with laboratory experiments are then described. The field data are of necessity limited and the interpretations subject to conceptual and many other kinds of uncertainties. Nevertheless, the field observations offer surprisingly strong tests of currently available thermodynamic data and alteration and transport models and the analogue analysis leads to specific recommendations for improving both data and models. Finally, the models calibrated by field observations at Poços de Caldas are applied to a hypothetical high-level waste repository to predict the near-field alteration and potential uranium transport over 10,000 years.

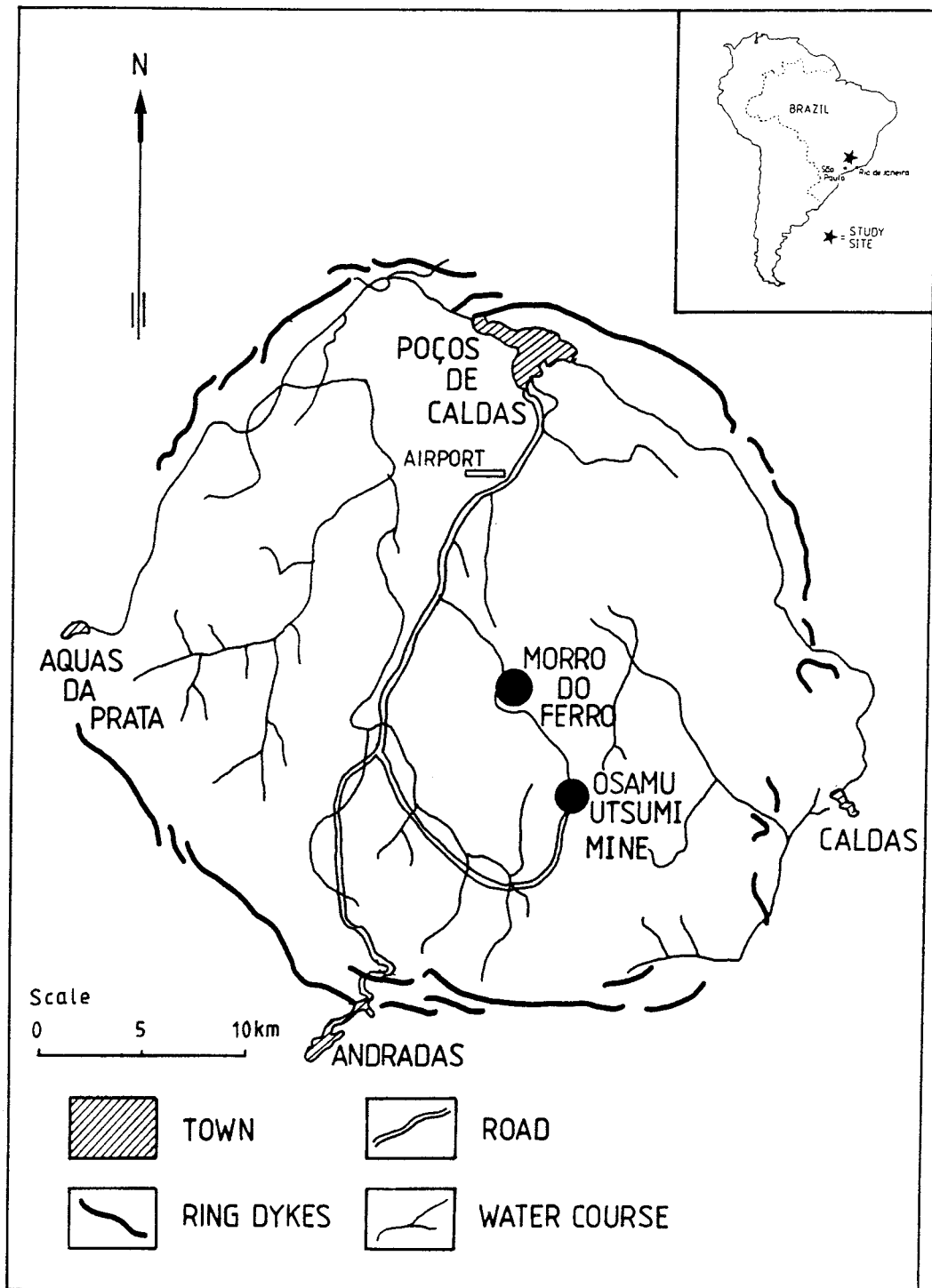


Figure 1. Location of the Osamu Utsumi mine natural analogue site.

2. Uranium mineralization at the Osamu Utsumi mine

2.1. The physical system

The first step in modelling is to place the mine location where most of the data have been collected in the context of the full mineralizing system. This is done in Figures 1-4.

Mineralization and alteration in and around the Osamu Utsumi mine occurred 76 Ma ago during a second pulse of syenitic ring dyke injection and resurgent doming of the 30-km-wide Poços de Caldas caldera (Schorsch and Shea; Shea, this report series; Reps. 1 and 4). The Osamu Utsumi mine (Fig. 2) is located in a relatively permeable breccia dyke of 0.5 kilometer diameter that lies adjacent to a small syenite intrusion (Fig. 3). The intrusion is the apophysis of a larger intrusion at depth. There has been significant erosion since the time of mineralization. Holmes et al. (this report series; Rep. 5) estimate an average erosion rate of ~12 m/Ma (10 to 50 m/Ma over 70 Ma) for a total erosion of 500 m. Neretnieks (this report series; Rep. 12) has pointed out that, taking into account the 30 ppm uranium left behind in the oxidized zone (that will be removed by erosion), the redox front must have migrated at least 0.5 km (and at least this much erosion must have occurred) to produce the uranium enrichment observed at the redox front.

Figure 4 shows a conservative (in the sense that the size of the intrusion is minimized) estimate of what the entire system might have looked like at the time of mineralization. A burial depth of 1.5 km has been assumed, showing no surface topography for the caldera walls etc. It is sobering to realize how little of the system it has been possible to sample from outcrop, mine workings and drilling (darker labeled “observations”). This is the first and perhaps most important conclusion to be reached from modelling; little is known about the system that produced the primary mineralization. It would probably be unrealistic to expect that this limited information could ever be expanded by enough deep drilling to provide the constraints required. Certainly, for this project, as much information as possible must be extracted from the spatially limited observations that are available.

Fortunately, adequate and varied chemical data exist in the “observation band” of Figure 4 and these data, especially when combined with physical and chemical modelling, can provide apparently strong constraints on the nature of the entire mineralizing system. In particular, viewed as an analogue experiment, observations at Poços de Caldas, limited though they are, can help to define and test chemical/physical models of what could occur in the vicinity of a high-level waste repository.

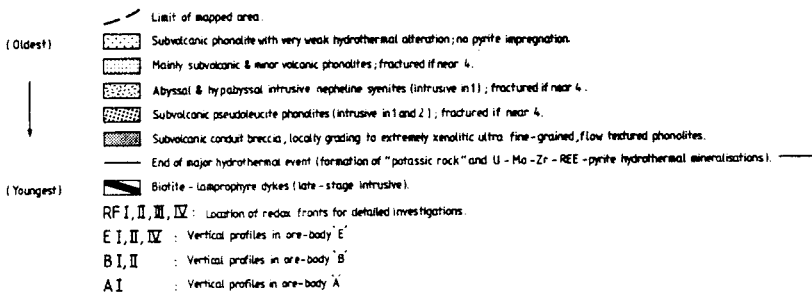
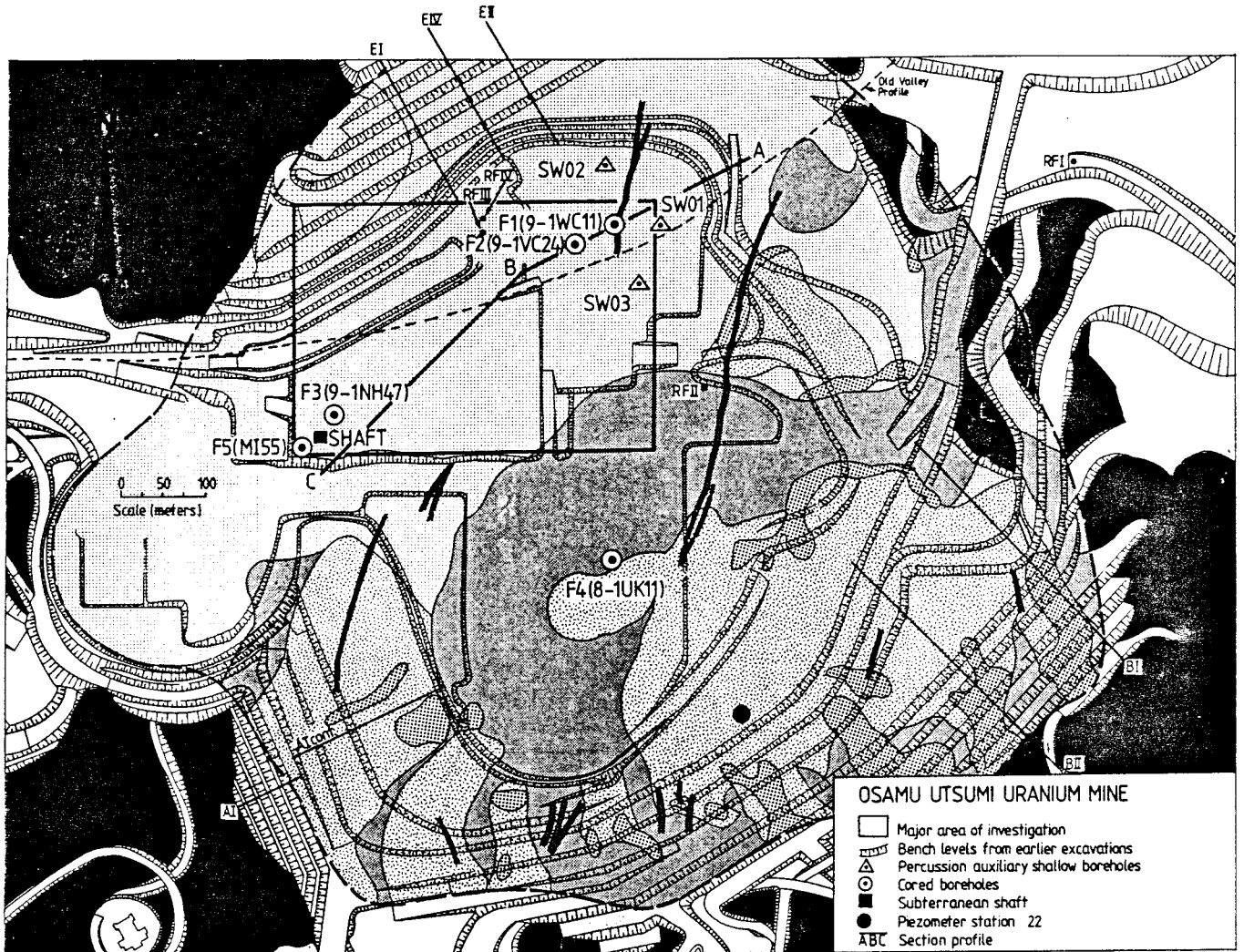


Figure 2. Osamu Utsumi mine showing the main geological subdivisions and the location of borehole F4(8-1UK11) drilled for hydrothermal studies.

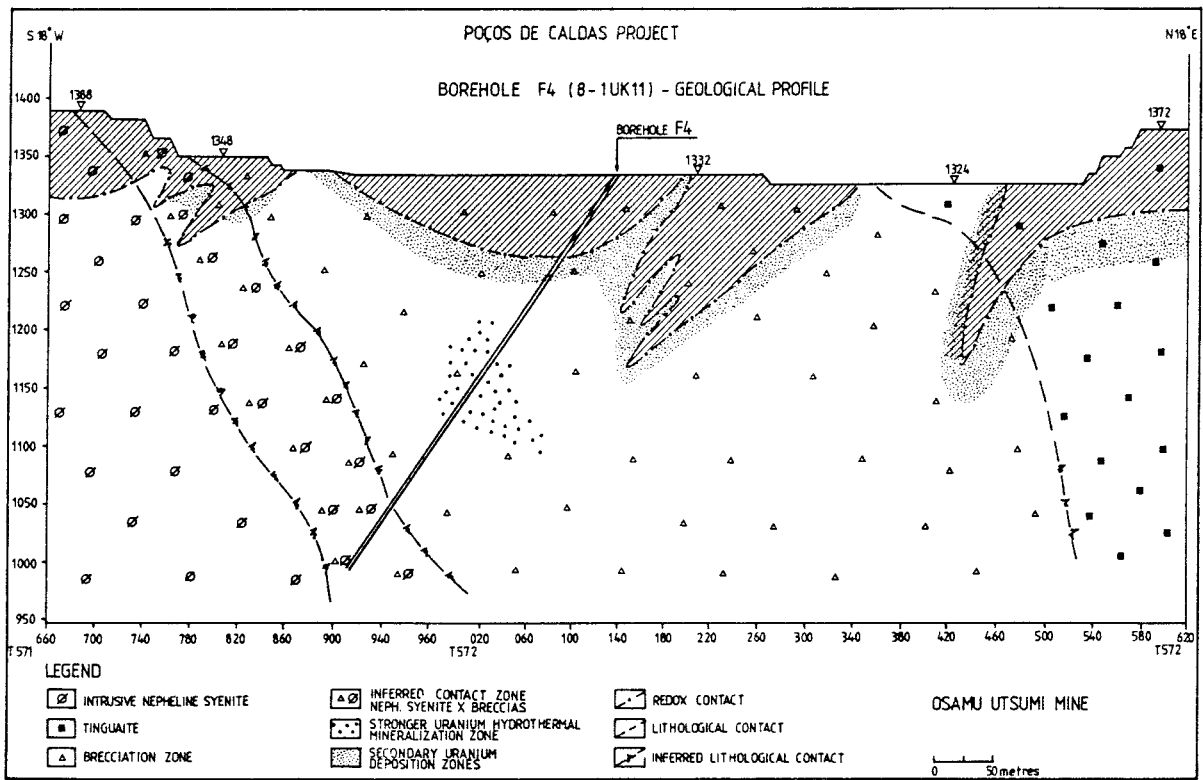


Figure 3. North-south cross-section of the Osamu Utsumi mine showing the relationship of borehole F4 with the breccia pipe and associated uranium mineralization.

MODEL GEOMETRY

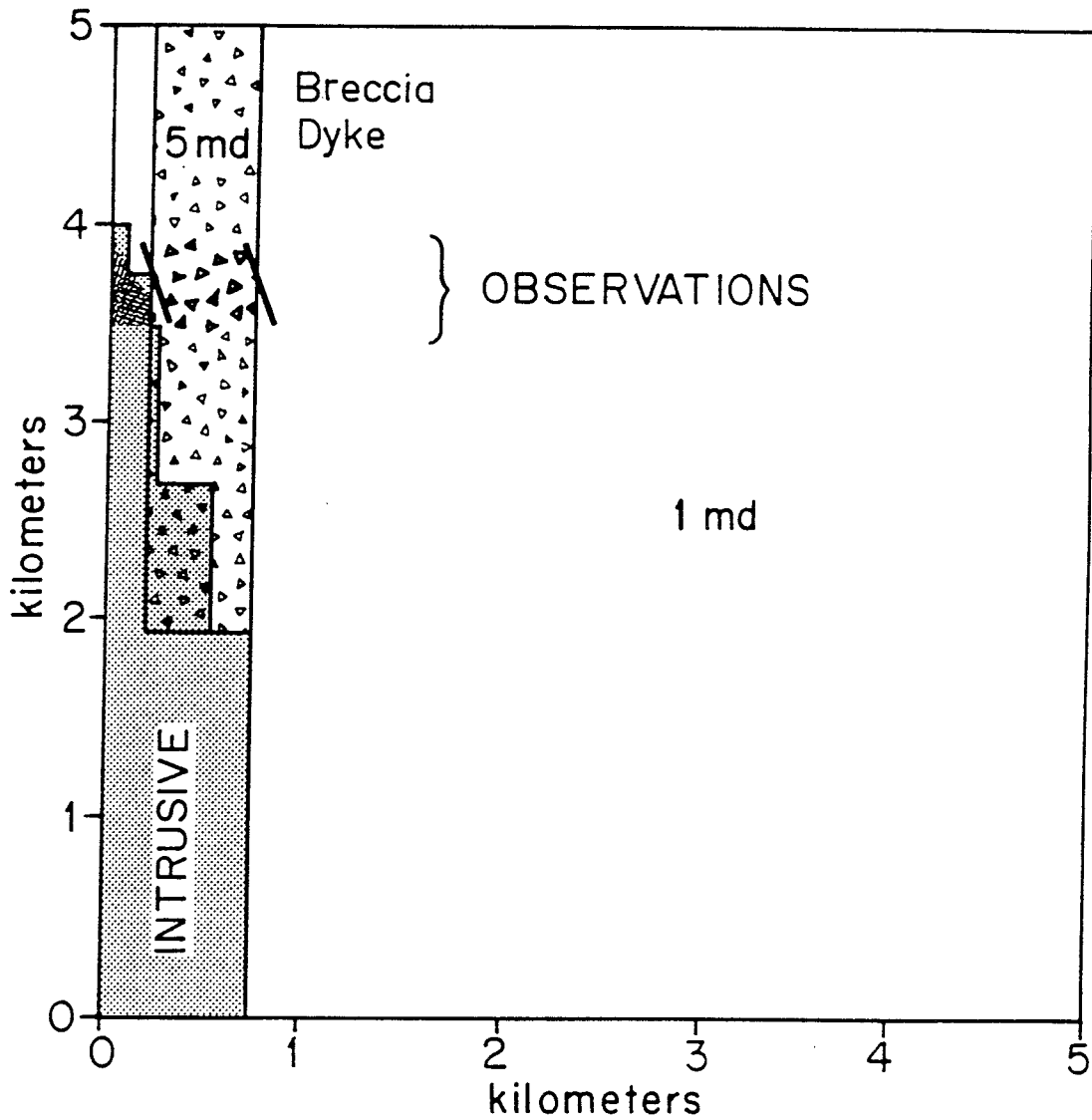


Figure 4. Hypothetical cross-section of the Osamu Utsumi mine showing a conservative estimate of what the entire system might have looked like at the time of mineralization and alteration. Observations from the open pit are limited to a thin band approx. 1 1/2 km below what was the surface at the time of mineralization.

2.2. Chemical changes

The reduced portions of the breccia pipe that hosts the Osamu Utsumi mine contain on average about 40 ppm by weight uranium, with local concentrations up to 200 ppm. The hydrothermal fluids that deposited this primary uranium mineralization also affected the whole-rock oxygen isotopic signature of the breccia pipe. Its present signature is quite uniform at $\delta^{18}\text{O} \sim 6.6 \pm 0.9\text{‰}$ (all δ -values relative to SMOW). The hydrogen isotopic signature of the breccia pipe shows a regular trend from -82 to -45‰ (Shea, this report series; Rep. 4). Unaltered syenites in the area have $\delta^{18}\text{O} = 8.5 \pm 1.1\text{‰}$ and $\delta\text{D} = -80 \pm 10\text{‰}$ (Shea, op. cit.). Thus, passage of the hydrothermal solutions through the breccia pipe depleted the rocks by a few parts ‰ in $\delta^{18}\text{O}$ and enriched the rock in δD at the same time that they deposited ~ 40 ppm U. Meteoric water at Poços de Caldas at the time of mineralization was preliminarily estimated to have had $\delta^{18}\text{O} \approx -4\text{‰}$ and $\delta\text{D} \approx -20\text{‰}$ (Shea, op. cit.). At moderate temperatures ($\sim 150^\circ\text{C}$), the hydrogen isotopic fractionation factor between water and rock is $\sim -30\text{‰}$. Thus the δD signature of the breccia pipe trends toward values ($\sim -50\text{‰}$) that would be in equilibrium with local meteoric water. There is no indication of a similar shift in $\delta^{18}\text{O}$ toward values of $\sim 0\text{‰}$ that would be in equilibrium with meteoric waters at $\sim 200^\circ\text{C}$; the $\delta^{18}\text{O}$ values cluster around 6.6‰ .

The most striking primary alteration, however, is chemical. Nepheline syenites in the breccia pipe are almost completely stripped of Na and their K content has been greatly increased. These changes are shown in Table I for average values reported in Waber *et al.* (this report series; Rep. 2). For subsequent reference, the change in moles per kilogram between unaltered and altered nepheline syenite is also listed in Table I.

The chemical changes inferred by comparing equal masses of altered and unaltered rock are, however, subject to several uncertainties. First, there is no way of knowing how accurately the unaltered samples represent the “predecessor” of the altered samples. The unaltered samples used in this study may be hydrated relative to other reported unaltered values for the Poços de Caldas Plateau (e.g. Waber *et al.*, this report series; Rep. 2), which suggests that hydration may be a more important part of the alteration than suggested by Table I. More importantly, the alteration process may have added (or removed) mass. For example, 70 grams of unaltered predecessor might correspond to 100 grams of altered product, with 30 grams introduced by the hydrothermal solution. Such a situation, which evidence presented below indicates was actually the case, suggests a mass transport very different from that deduced by

comparing the compositions of equal masses of altered and unaltered rock as in Table I.

TABLE I

Comparison of unaltered nepheline syenites in the Poços de Caldas Plateau and altered F4 drillcore suggests the alteration consists mainly of removal of Na and addition of K. Modal compositions are listed in grams of oxide components per 100 grams of sample in columns 2 and 3. Unaltered nepheline syenite data are the average of samples NS 1,4,6,7 from Waber *et al.* (this report series; Rep. 2). Altered data (breccia) are an average of 9 samples: F4-91, 123, 129, 265 and F4-413-AA, AB, AC, AD and AE, from Waber *et al.* (op. cit.). Samples F4-19, 22, 30 were omitted because they are oxidized and F4-107 is omitted because it is a different rock type (foyaite) with distinct chemistry. Note Fe₂O₃(tot) is total iron reported as Fe₂O₃. The chemical change is given in columns 4 and 5.

Mode			Chemical	Alteration in moles added
Component	Unaltered	Breccia	Change in g/100g	per kg rock (basis component)
Na ₂ O	7.21	0.62	-6.59	-2.13 (Na)
CaO	1.79	0.83	-0.96	-0.17 (Ca)
MgO	0.37	0.16	-0.21	-0.05 (Mg)
TiO ₂	0.78	0.63	-0.15	-0.02 (Ti)
P ₂ O ₅	0.11	0.09	-0.02	-0.003 (P)
Fe ₂ O ₃ (tot)	4.11	4.29	0.18	0.023 (Fe _{tot})
H ₂ O	2.43	3.02	0.59	0.033 (H ₂ O)
MnO	0.26	0.57	0.31	0.036 (Mn)
Al ₂ O ₃	19.32	19.57	0.25	0.045 (Al)
CO ₂		1.02		
SiO ₂	52.53	53.94	1.41	0.23 (SiO ₂)
K ₂ O	7.88	12.95	3.81	0.809 (K)

That mass has, indeed, been added to the unaltered protolith is suggested by the strong correlation between SiO₂ and K₂O in the altered samples. This correlation was pointed out by Waber *et al.* (this report series; Rep. 2). Their plot shows unambiguously that SiO₂ is added to the rock during alteration at a faster rate than K₂O. This magnitude of silica addition is not reflected in the equal mass comparisons of Table I and clearly shows that a more sophisticated analysis is necessary.

Such an analysis can be made if at least one of the analyzed components was immobile during alteration and of relatively uniform concentration in the unaltered nepheline syenite. TiO₂, MgO, and P₂O₅ are all good candidates. TiO₂ was selected and the weight percent oxide analyses on samples listed in Table I were converted to moles

oxide per kilogram rock, and then the number of moles were adjusted so that each sample contained the same number (0.076) of moles of TiO_2 . This is a simple form of Gresen analysis (e.g. Appleyard, 1980; Babcock, 1973; Gresens, 1967). Regression of the analytical data adjusted in this fashion against K_2O shows that many of the oxide components vary with K_2O ; others, however, do not. (Figs. 5a, 5b). Without TiO_2 adjustment, only SiO_2 varies with K_2O . The greatly increased coherency of the data justifies the assumption of TiO_2 immobility.

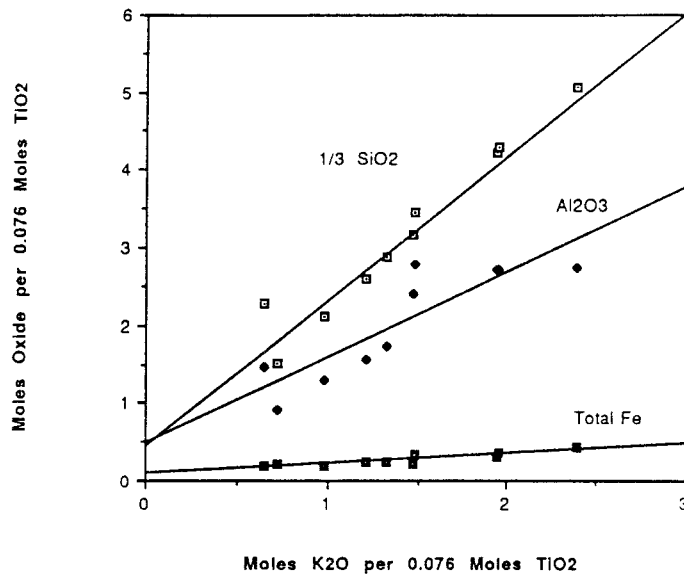
The following rates of addition (or subtraction) of oxide components relative to K_2O were indicated by the analysis: $\text{SiO}_2 = 5.8 \pm 0.5$ moles/mole K_2O (correlation coefficient 0.97), $\text{Al}_2\text{O}_3 = 1.1 \pm 0.2$ moles/mole K_2O (correlation coefficient 0.87), $\text{Fe}_2\text{O}_3 = 0.12 \pm 0.02$ moles/mole K_2O (correlation coefficient 0.88), $\text{H}_2\text{O} = 1.14 \pm 0.38$ moles/mole K_2O (correlation coefficient 0.726) and $\text{CaO} = 0.16 \pm 0.11$ moles/mole K_2O (correlation coefficient 0.452). Na_2O dropped very rapidly with alteration. As a consequence, Na_2O had a very low and near constant value in almost all the altered samples. The amount of Na_2O in unaltered plateau samples suggests the change relative to K_2O was about -2 moles/mole. All of the other elements had low correlation coefficients (less than 0.31 and slopes equal to zero within error limits).

Thus, in a reference frame of a constant number of TiO_2 atoms, an increase of 0.6 moles K_2O (or 1.2 moles K^+ , i.e. a rough estimate of the average change in K_2O ; see Table I and Fig. 5a for the breccia) requires a metasomatic flux to the altered rock of 3.46 mol SiO_2 , 1.32 mol Al^{+++} , 0.15 mol. Fe, 0.68 mol H_2O , 0.09 mol Ca^{++} and -2.4 mol Na^+ . These Gresen analysis estimates of element fluxes to the breccia are listed in the last column of Table III.

2.3. Petrologic changes

Alteration can also be viewed in mineralogical terms and the chemical implications of the petrography must be consistent with the changes inferred from the chemical analyses. Petrographic investigations by Waber *et al.* (this report series; Rep. 2) showed that the alteration in the breccia could be viewed simply as conversion of the originally present nepheline, sanidine and aegirine augite to kaolinite, illite and microcline, as indicated in Table II. The chemical compositions shown in Table II have been measured by microprobe (product minerals) or estimated (original minerals).

(a) Oxides Correlated with K₂O



(b) Water and Non-Correlating Oxides

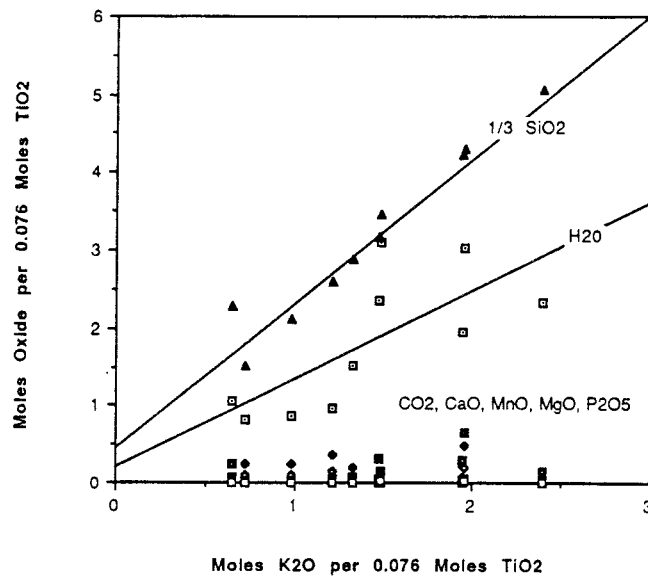


Figure 5. Plots of regression of oxide rock components against K₂O: a) oxides correlated with K₂O and b) water and non-correlating oxides. Rock compositions were normalized before regression so that all samples contained 0.076 moles of TiO (a simple kind of Gresen correction). Oxide components without regression lines show poor correlation and, within error limits, zero slopes.

TABLE II

Petrologic alteration of the breccia (F4 borehole) samples. The minor alteration phases are somewhat arbitrary.

Unaltered Poços de Caldas Plateau nepheline syenites		
30 wt. %	Nepheline	$\text{Na}_{0.75}\text{K}_{0.25}\text{AlSiO}_4$
60 wt. %	High sanidine	$\text{K}_{0.6}\text{Na}_{0.4}\text{Si}_3\text{O}_8$
10 wt. %	Aegirine augite	$\text{NaCa}_{0.1}\text{Mg}_{0.1}\text{Fe}^{3+}_{0.866}\text{Si}_2\text{O}_6$
Altered Poços de Caldas breccias		
23 wt. %	Illite	$\text{K}_{0.3}\text{Mg}_{0.05}\text{Fe}^{2+}_{0.125}\text{Fe}^{3+}_{0.15}\text{Al}_{1.8}\text{Si}_{3.875}\text{O}_{10}(\text{OH})_2$
60 wt. %	Max. microcline	KAlSi_3O_8
14 wt. %	Kaolinite	$\text{Al}_2\text{Si}_2\text{O}_5(\text{OH})_4$
1 wt. %	14Å-Daphnite	$[\text{Fe}^{2+}\text{Al}][\text{AlSi}_3\text{O}_{10}](\text{OH})_8$
1 wt. %	Pyrite	FeS_2
0.5 wt. %	Fluorite	CaF
0.5 wt. %	Hematite	Fe_2O_3

The basis species changes (in moles per kg rock) required by the mineralogical changes shown in Table II are given in Table III and are compared to the chemical changes deduced above. These changes were calculated by multiplying the stoichiometric matrix (which describes the minerals in Table II in basis species components) by the modal mass fractions listed in column 1 of Table II (with the modes of the minerals destroyed by alteration taken to be negative and reduced by the ratio of altered to unaltered rock mass). For example, the second column in Table III gives the metasomatic flux in moles of basis species per kilogram of product if 100 g of protolith is altered to 100 g of product. The third column gives the metasomatic flux required to alter 70 g of protolith to 100 g of product.

The last column in Table III gives the metasomatic flux determined from the Gresen analysis discussed above, assuming the breccia is on average enriched in K^+ by 0.6 moles per kilogram. It can be seen that the petrographic observations are compatible with the observed chemical changes provided that the rock mass increased by about 30% during hydrothermal alteration. Only if this is the case are the ratios of added silica, total iron and aluminium deduced from the observed mineralogical change compatible with the ratios of these changes deduced from the Gresen analysis.

TABLE III

Flux of basis species to the rock (in moles per kg rock) required by mineralogical changes in Table II assuming 100 g and 70 g protolith per 100 g of total altered product compared to chemical changes estimated by Gresen analysis as discussed in text.

Basis Species	100 g protolith for 100 g product	70 g protolith for 100 g product	Chemical change of basis components (Gresen analysis)
Na ⁺	-2.86	-2.00	- -2.40
Mg ⁺⁺	-0.013	-0.000	0 0 (Ti) 0 (P) 0 (Mn)
Ca ⁺⁺	0.006	0.02	0.09
F ⁻	0.10	0.10	
Fe _{tot}	0.00	0.12	0.15 (Fe _{tot})
HS ⁻	0.17	0.17	0.68 (H ₂ O)
K ⁺	0.50	1.05	1.20
Al ⁺⁺⁺	0.10	1.38	1.50
SiO ₂ (aq)	0.40	3.26	3.46

For about 30 wt.% addition of hydrothermal products, the chemical and petrologic analyses agree well. The agreement can be improved by changing slightly the amount of minor phases such as pyrite, etc. produced. The important conclusion to be drawn at this point is that the petrologic observations and observed chemical changes are quite compatible with one another provided the rock mass has been increased by the hydrothermal alteration. Silica, potassium, sulfur and uranium have been added to the rock by hydrothermal fluids and sodium has been removed. If the fluxes to the rock in Table III are taken as a good measure of what has occurred, and a 500-m-thick layer of the Poços breccia pipe with density 2.5 g/cc was thus altered, the hydrothermal fluid must have provided (or removed) the quantities of constituents listed in Table IV.

TABLE IV

Estimates of the moles of major constituents deposited or removed by the hydrothermal fluid passing through a 500-m-thick section of the Poços de Caldas breccia pipe at the Osamu Utsumi mine. Additions to the rock are positive and the units are moles per cm² cross-section of the breccia pipe. A breccia density of 2.5 g/cc is assumed.

Element	moles/kg breccia added	moles/cm ² in 500 m thick layer breccia
Na	-2.40	-300
U	2x10 ⁻⁴	0.025
Ca	0.09	11
F	0.10	13
Fe _{tot}	0.15	19
Al	1.2	150
K	1.2	150
SiO ₂	3.46	432

2.4. Other observations

Fluid inclusions have been observed and studied in fluorite deposited during primary mineralization. These inclusions homogenize at 200–220°C and are of two distinct types. The first two populations have about 10 vol.% vapor phase and ~7 wt.% salinity (believed to be mostly KCl). These inclusions are believed to have been trapped during the early and intermediate stages of alteration. In the later, third fluid inclusion population, 90 vol.% vapor inclusions coexist with liquid inclusions of high salinity. This mix of vapor and liquid-dominated inclusions suggests boiling of the warm upwelling solutions and concentration of salts in the residual liquid phase (Waber *et al.*, this report series; Rep. 2).

Geological and petrologic studies of the breccia (Waber *et al.*; *op. cit.*) indicate that the rock alteration occurred in two stages. The first stage, referred to as the “auto-alteration” or metamorphic stage, affected the mineralogy but not the bulk chemistry. It occurred between ~700°C (magma temperatures) and ≥350°C. The second, metasomatic stage of alteration introduced K, S and U and removed Na. During this stage, the rock temperature was ≤350°C. This metasomatic stage may have been thermally distinct in the sense that it involved heating and then cooling. It could also simply represent the time when circulating fluids first began to interact significantly with the steadily cooling rock mass.

Permeability measurements have been made in a number of boreholes in the area. Permeability typically decreases from ~10 darcies (10^{-4}m s^{-1}) to 10 to 100 millidarcies at depths of a few tens of meters (Holmes *et al.*, this report series; Rep. 5). (See for example measurements in F1, F2 and a 100-m borehole in the bottom of the open mine pit.)

3. Calculation of the fluid circulation responsible for uranium mineralization and alteration at the Osamu Utsumi mine

3.1. Base physical model of fluid circulation

Taking the above geological, geochemical and geotechnical information into account, calculations have been made of the hydrologic flow the small intrusive body would produce in an adjacent 500-m-wide breccia pipe extending from the surface to 3 km depth as shown in Figure 4. The permeability of the intrusion (at $T < 300^\circ\text{C}$) and host rock (excluding the breccia pipe) was taken to be 1 millidarcy. The breccia pipe permeability was 5 millidarcies. The central temperature of the intrusion was 700°C . The intrusion was cooled for 1000 years without any convection (to smooth the intrusion outline and increase computational stability and also to simulate the auto-alteration or metamorphic stage of alteration). The permeability of the intrusion was reduced exponentially at temperatures above 300°C , as has been previously indicated to be appropriate by studies of other hydrothermal systems (see Cathles, 1983). This is also in accordance with the temperature ceiling on metamorphic alteration inferred from the studies of petrologic alteration at the Osamu Utsumi mine mentioned above. Free flow was allowed through the top surface. No flow crossed vertical planes 5 km from the axis of the intrusion and no flow was allowed across the basal boundary which was taken at 5 km depth. The surface pressure (300 bars) was sufficient to prevent boiling. A normal hydrostatic pressure gradient was assumed to be maintained by fluid flow throughout the system.

The coupled fluid convection and temperature equations were solved by a Douglas Rachford alternating direction implicit finite difference scheme, which is an updated version of that described in detail in Cathles (1977).

The results of the fluid flow calculations are shown in Figures 6–9. The thermal and convective evolution for the first 10,000 years is shown in Figure 6. About 2000 years of convection (3000 years elapsed model time) is required for the entire breccia pipe

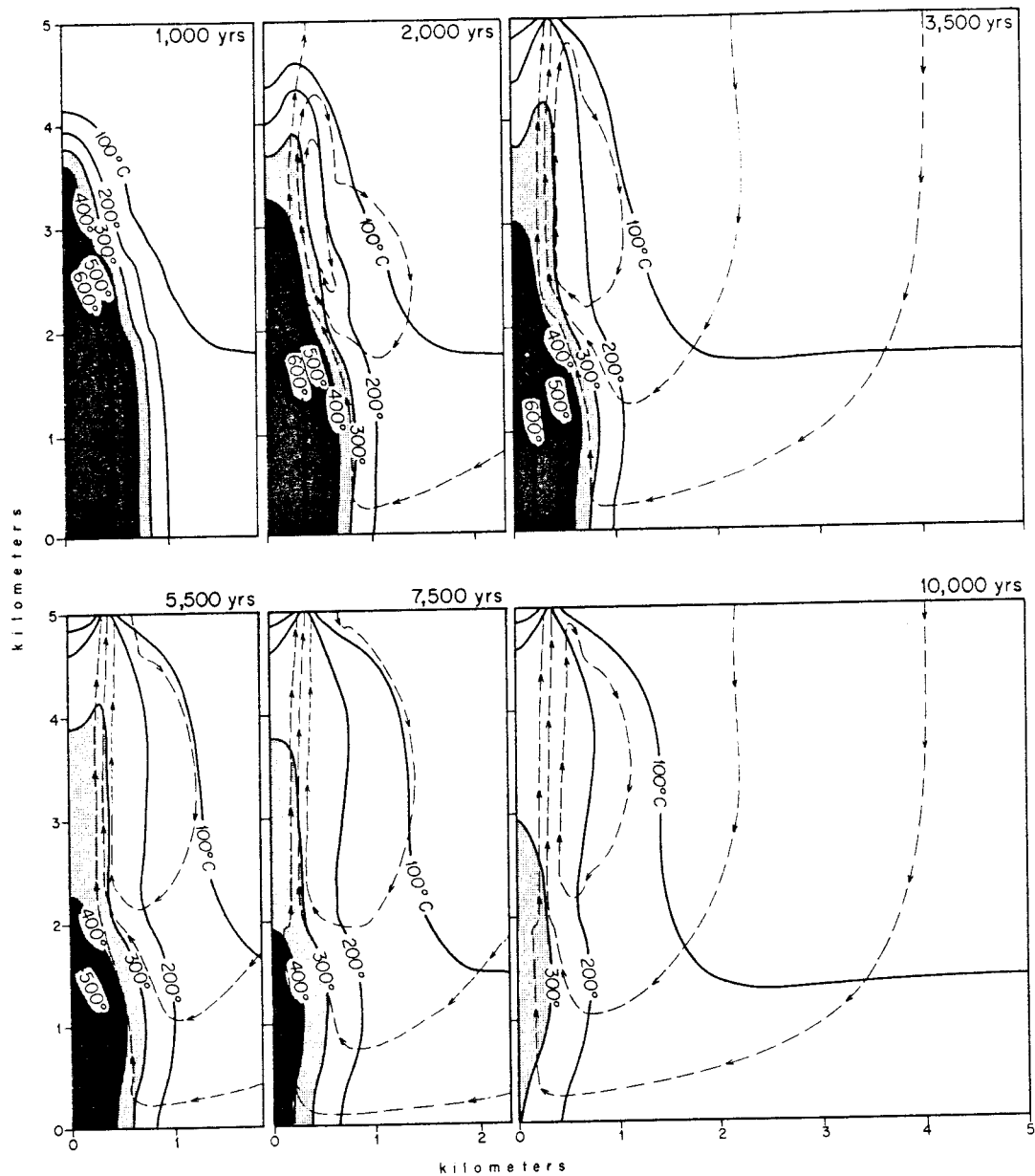


Figure 6. Cross-sections 1000 to 10,000 years after intrusion showing the progressive cooling of the intrusion depicted in Figure 4 by groundwater convection. The temperature of the initially 700°C intrusion is indicated by solid contours. Streamlines indicating the direction of fluid flow are shown with dashed lines and arrows. The general permeability is 1 millidarcy, except for the breccia pipe which has a permeability of 5 millidarcies and the intrusion whose permeability decreases exponentially with temperature for temperatures greater than 300°C.

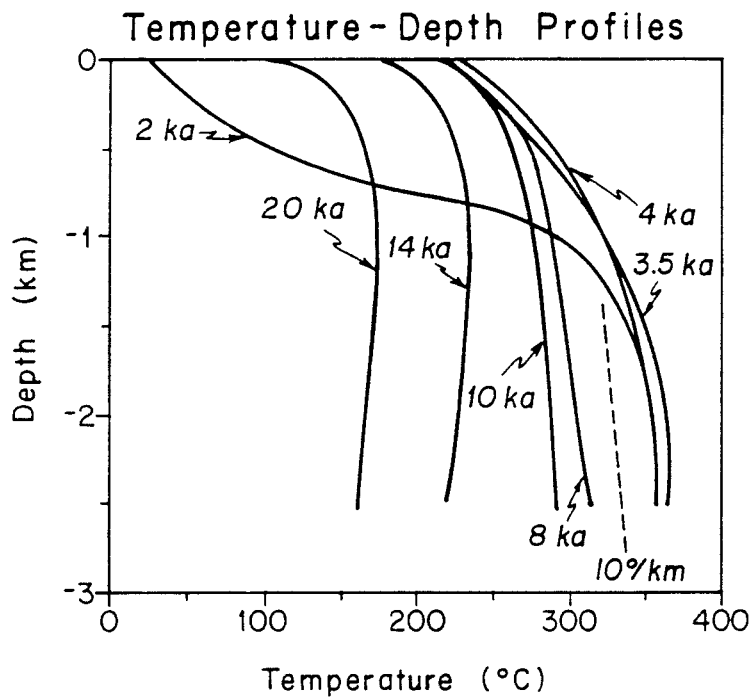


Figure 7. Profiles through the highest flow parts of the breccia pipe. Even with no boiling, as assumed in calculations shown in Figure 6, the temperature drops by about 11°/km as the fluids move upwards through the pipe.

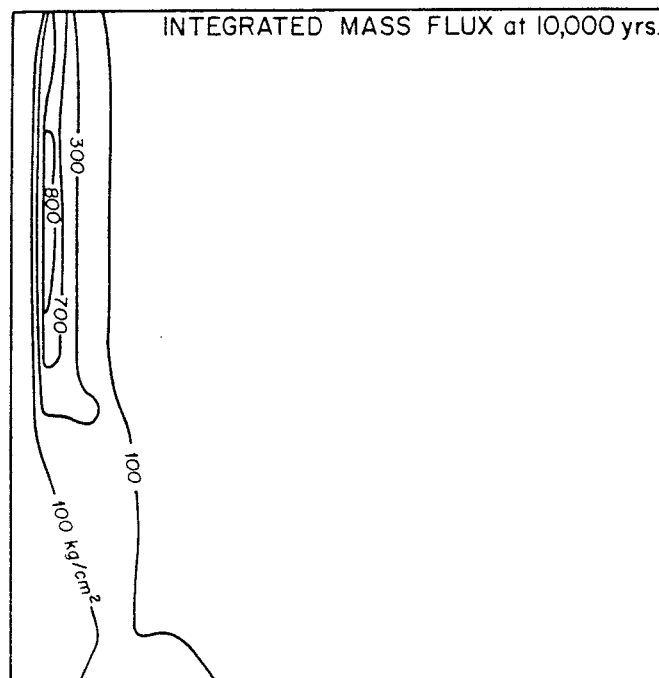


Figure 8. The total fluid flux after 10,000 years of convective cooling. The inner parts of the breccia pipe have seen the passage of over 800 kilograms of hydrothermal fluid per square centimeter plan cross-section of the pipe.

to heat up and for high-temperature fluids to reach the surface. Active convection through the breccia pipe occurs from 1000 to 13,000 years. By 14,000 years, however, the intrusion is largely heat-depleted and the lower 2/3 of the breccia pipe has substantially cooled.

Figure 7 shows temperature profiles along streamlines through the high flow part of breccia pipe. As long as the intrusion remains warmer than the surrounding areas, fluid movement through the pipe and convection adjacent to it combine to cause the fluids in the pipe to move down a slight temperature gradient of $\sim 11^{\circ}\text{C}/\text{km}$. Fluids move up a temperature gradient in the pipe only in the very last stages of cooling when the thermal anomaly retreats up the pipe to fully disappear.

Flow is strongly concentrated in the pipe. The integrated fluid mass flux at 10,000 years is shown in Figure 8. This figure shows that the mass flux is generally less than $\sim 50 \text{ kg}/\text{cm}^2$, but in parts of the pipe the integrated flux exceeds $700 \text{ kg}/\text{cm}^2$. The focussing of fluid through the pipe is impressive. Figure 9 shows the maximum integrated mass flux in the breccia pipe at 2 km depth as a function of time. The amount of circulation in the pipe at 1 km depth is similar. By the time the intrusive has cooled, over 1000 kg of hydrothermal solution has passed through each cm^2 of cross-sectional area in the high flow portions of the pipe. Note, as shown in Figure 8, that there is a natural tendency for the flow to concentrate in parts of the pipe. This natural tendency could be augmented by any permeability variations within the pipe.

The amount of fluid circulation through the breccia pipe at the Osamu Utsumi mine depends on many factors. The most important are the size and geometry of the intrusion(s) driving the hydrothermal circulation and the contrast in permeability between the breccia pipes and the surrounding host. If the size of the intrusion were doubled, twice as much hydrothermal solution would circulate through the pipe. If the pipe were more permeable relative to its surroundings, more flow would be attracted to it and the mass flux might be concentrated in a smaller fraction of the pipe. Beyond a certain point, increasing the pipe permeability will not attract further fluid to the pipe as a whole. If the permeability of the pipe and its surroundings were increased by the same factor, the mass flux through the pipe would not change; the intrusion would just cool faster. Clearly a great many calculations could be presented. The system is, however, unconstrained enough, that it is best to proceed on the basis of the reasonable physical model just developed. The plausibility of increasing the flow through the pipe will be addressed after the flow requirements of chemical alteration have been assessed.

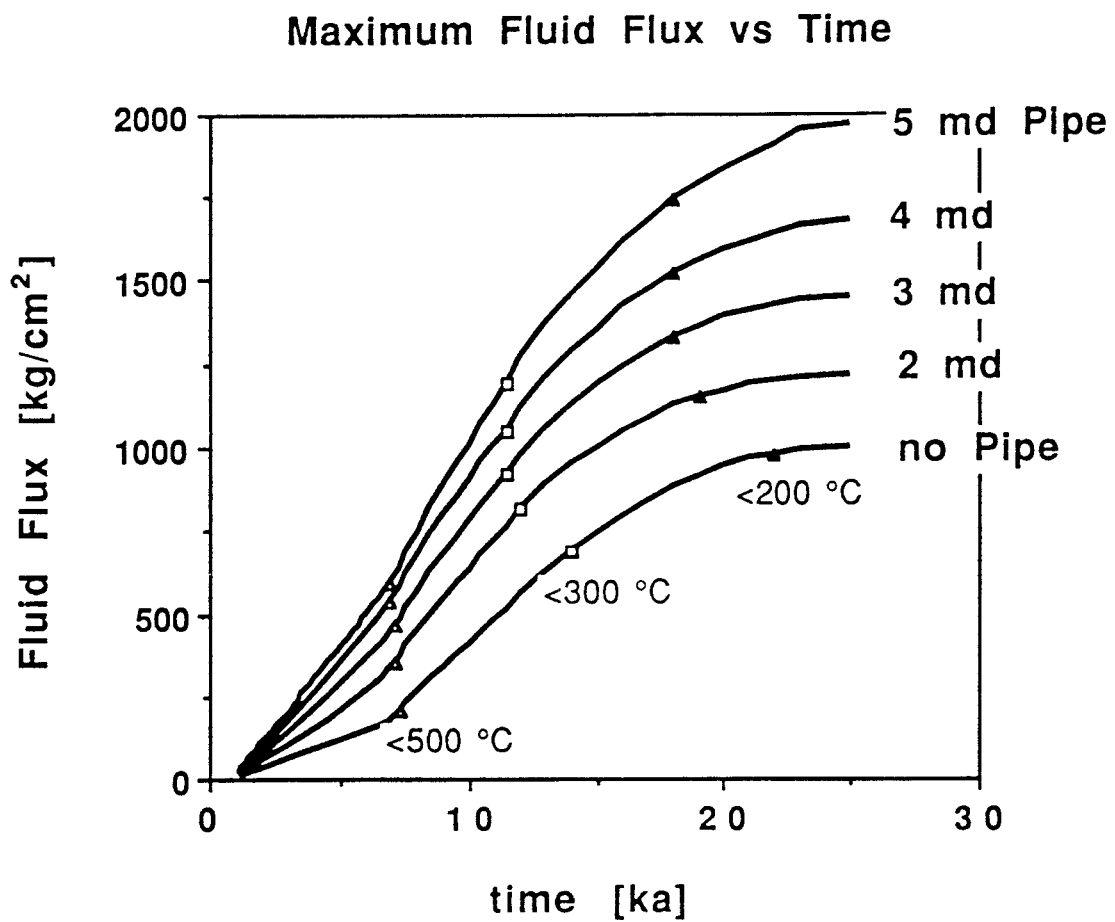


Figure 9. The maximum integrated fluid flux at any point in the breccia pipe as a function of time. Convection starts after 1000 years of conductive cooling. Points at which the maximum temperature of the intrusion falls below 500°, 300° and 200°C are indicated on each curve.

3.2. Circulation required for the low-grade hydrothermal uranium mineralization

The most obvious question in a study addressing natural radionuclide transport is whether the amount of hydrothermal circulation identified in the base physical model can account for the low-grade hydrothermal uranium concentration of ~50 ppm observed in the Osamu Utsumi breccia pipe. Here, the value of the analogue approach to evaluating geochemical data is immediately apparent.

Estimates of the solubility of uranium in natural, near-neutral hydrothermal solutions differ by many orders of magnitude. On the one hand, the EQ3 database and experiments by Lemoine, cited in a review by Kertes and Guillaumont (1985), suggest that the solubility of uranium (say by dissolution of uraninite) is 8.4 to 21×10^{-5} molal at 300°C and strongly temperature-dependent. On the other hand, the most recently published experimental study (Parks and Pohl, 1988) found the hydrothermal solubility of uraninite to be 3.3×10^{-10} molal and both temperature- and pH-independent (near-neutral pH). There is general agreement that the main complex of uranium is $\text{U}(\text{OH})_4$, so the difference apparently resides entirely in the dissolution log K of uranium minerals.

The Lemoine solubilities are quite compatible with the base physical model for fluid flow through the breccia at the Osamu Utsumi mine. The 0.025 moles of uranium contained per square centimeter cross-section through a 500 m mineralized portion of the pipe could be supplied by between 119 and 297 kg of hydrothermal solution if all the uranium were precipitated and the solution was saturated in uranium at 300°C .

This is less than the $\sim 1000 \text{ kg/cm}^2$ of hydrothermal solution the base model suggests to have passed through the pipe (Fig. 9). Furthermore, the strong dependence of uranium solubility on temperature indicated by Lemoine's experiments would provide a natural mechanism for uranium precipitation as the solutions cooled moving up the pipe.

On the other hand, it is very hard to see how the breccia pipe at the Osamu Utsumi mine could have been mineralized if the Parks and Pohl solubility is appropriate. Firstly, even if all the uranium were somehow precipitated, $\sim 7.5 \times 10^7 \text{ kg/cm}^2$ of hydrothermal solution would require to pass through the breccia pipe. This is ~ 5 orders of magnitude greater than indicated by the base model. Although it could be argued that an increase of two or three orders of magnitude is possible, a five order of magnitude increase is not geologically plausible. This will be discussed further below. Secondly, if there is no dependence of uranium solubility on temperature as indicated

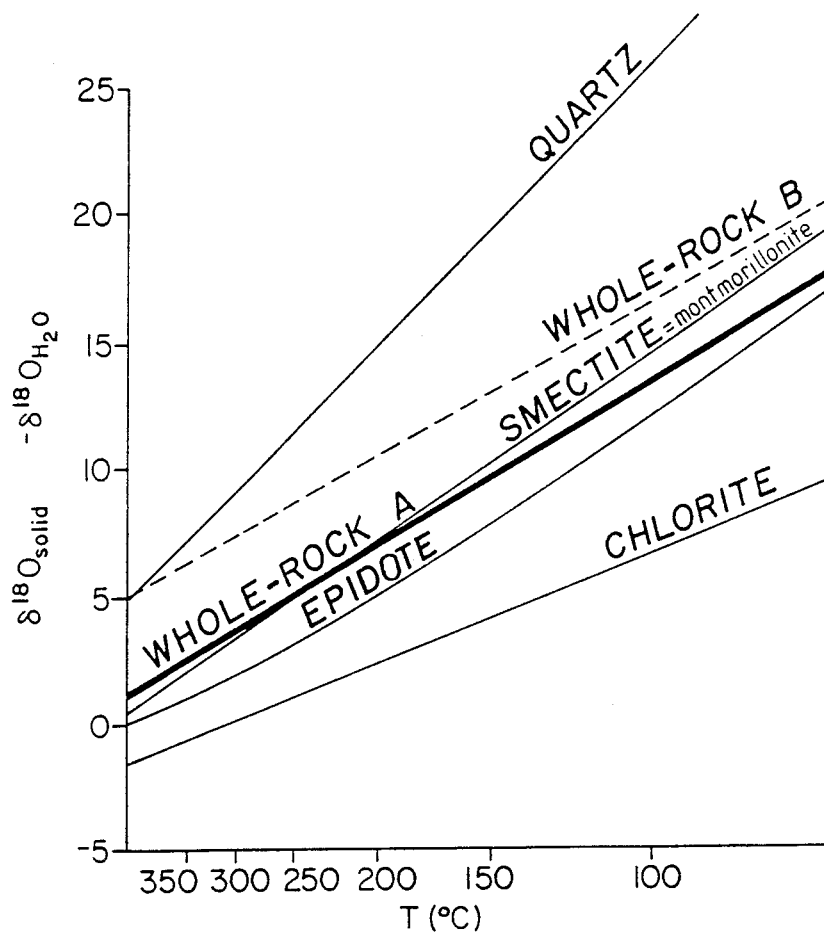


Figure 10. The whole-rock oxygen isotope fractionation curve used in calculating the whole-rock oxygen isotopic alteration shown in Figure 11 is compared to the isotopic fractionation curves for various minerals relative to water. Isotopic alteration depends almost entirely on the slope of the fractionation curve and is nearly identical for the dotted whole-rock curve. Whole-rock curves are discussed in the text. Whole-rock A was used in the calculations presented. Mineral curves are shown to provide a broader context for the whole-rock data. (Sources: see Taylor, 1979; Friedman and O'Neil, 1977.)

by Parks and Pohl, there is no obvious mechanism for uranium precipitation in some particular subsurface section of the pipe.

The Osamu Utsumi mine low-grade hydrothermal mineralization thus suggests that the uranium solubilities of Parks and Pohl are too small by several orders of magnitude and that Lemoine's solubility data may be more appropriate for natural environments.

3.3. Circulation required for isotopic alteration

An isotopic alteration model can be superimposed on the fluid and temperature evolution indicated by the base model shown in Figure 6 and the oxygen isotopic alteration of the system predicted. The oxygen isotopic model is described in Cathles (1983) and was calculated here for the whole-rock/water fractionation curve shown in Figure 10. In the models, the whole-rock oxygen isotopic signature was taken to be 10‰ and the local meteoric water entering the top surface to be -4‰, based upon our preliminary estimate using the plot of Sheppard (1986). The calculated change in isotopic signature after 10,000 years (9000 years of convective cooling) is shown in Figure 11. The use of isotopic data for waters collected in the Osamu Utsumi mine and the immediate vicinity exhibit $\delta^{18}\text{O} = -7.5\text{‰}$. The use of these values in our model calculations would not significantly affect the results of our interpretations.

The evolution of the rock oxygen isotopic signature follows a similar pattern for all intrusives cooling by convective circulation. A complete discussion is given in Cathles (1983). At Poços de Caldas, the light alteration tongue originating at the deep margin of the intrusive heat source has entered the breccia pipe by 10,000 years. At the level of the Osamu Utsumi mine, however, the oxygen isotopic shift is small. It is about the same after full cooling; in fact the negative isotopic shift is partly erased in the last stages of cooling. Since only a slight negative oxygen isotopic shift is observed in the breccia pipe at the Osamu Utsumi mine, the base physical model is compatible with the observed oxygen isotope alteration. It may be noted that the calculated oxygen isotopic alteration depends only very slightly on the particular fractionation curve chosen. For example, the results were almost identical when the dotted fractionation curve B in Figure 10 was used rather than the solid curve A.

The change in hydrogen isotopic signature in the pipe is expected to be much more rapid than, and of a different character to, the oxygen isotopic alteration. The oxygen isotopic alteration in the breccia pipe is related to the circulation of water up a steep temperature gradient at the deep margin of the intrusive heat source. The fluid is in

OXYGEN ISOTOPIC ALTERATION AT 10,000 YEARS

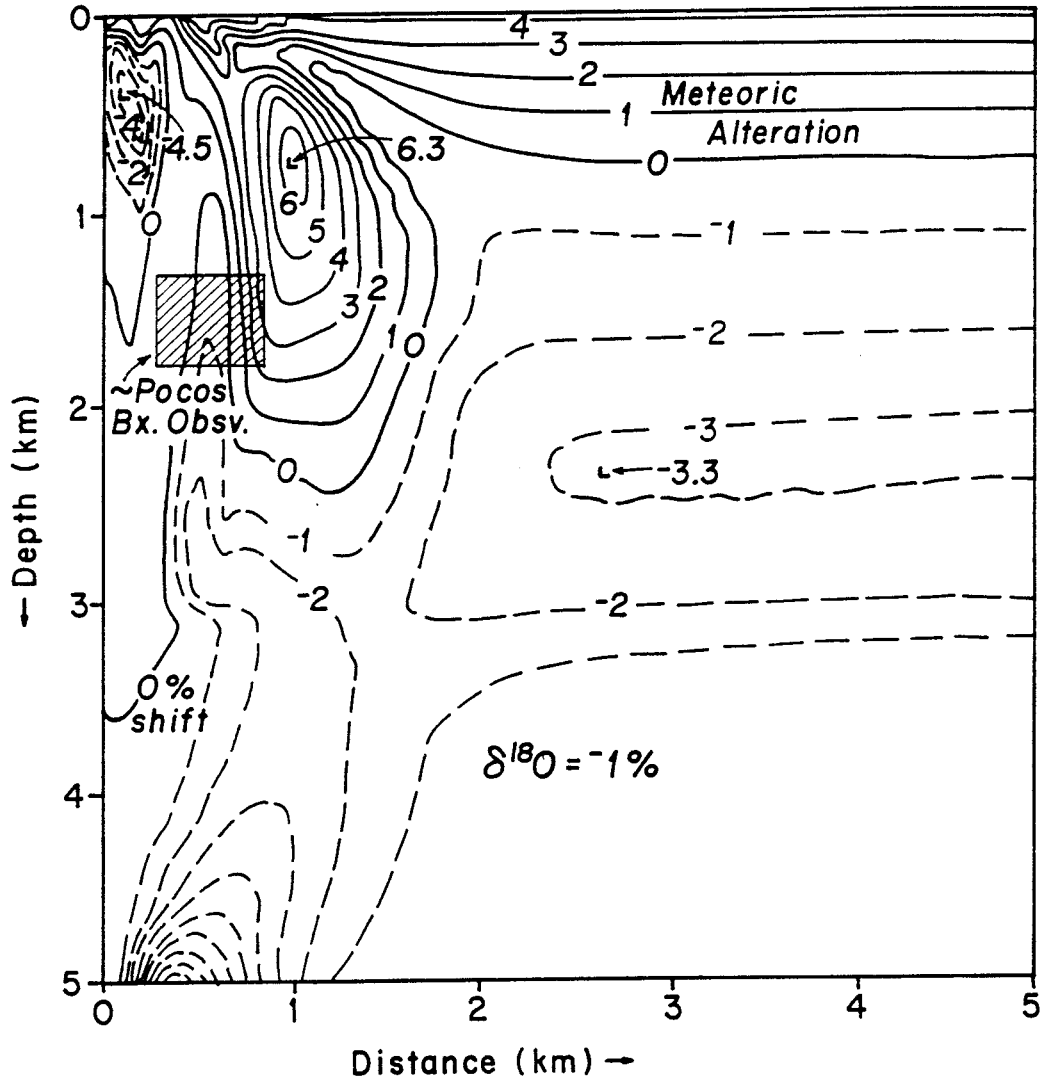


Figure 11. Shift in whole-rock oxygen isotopic signature of the rock caused by the convective circulation of meteoric waters entering the upper left hand surface at -4‰ . The "meteoric alteration" near the surface in inflow areas is the result of light meteoric waters equilibrating with rock at the rate kinetically allowed. Alterations elsewhere are mainly the result of fluids circulating up a temperature gradient as they move to greater depths and as they approach the intrusion (light isotopic shift). Notice that the rocks in the Poços de Caldas breccia pipe are only very slightly shifted to lighter isotopic signatures as observed at the Osamu Utsumi mine.

oxygen isotopic equilibrium with the nepheline syenite; the oxygen isotopic signature of the meteoric recharge water has been completely erased by water-rock equilibration. An oxygen isotopic alteration front associated with meteoric water intake is present, but it remains within 1 km of the surface where recharge is taking place (see zone above 0‰ contour in Figure 11, labeled meteoric alteration).

Hydrogen isotopic alteration is of a different character, primarily because the meteoric hydrogen isotopic alteration front moves much more rapidly through the system. Water contains 110 moles of hydrogen per kilogram and altered Poços de Caldas nepheline syenites 2.7 moles of hydrogen per kilogram of rock, whereas for oxygen the corresponding numbers are 55 and 37 moles per kilogram respectively. The alteration front associated with meteoric hydrogen thus sweeps through the convective system ~28 times faster than the meteoric oxygen isotopic front. The meteoric hydrogen isotopic front corresponding to the 1 km advance of the meteoric oxygen isotopic front in Figure 11 would lie 28 km downstream. Since the convective path is less than 15 km, the meteoric hydrogen isotopic front would have swept through the model system in the first 5500 years. The fractionation between rock and water is about -30‰ and relatively independent of temperature (Taylor, 1979; Cole *et al.*, 1987). Thus if the meteoric water 76 Ma ago at Poços de Caldas were similar to today (-20‰), the rock should show a shift towards values of -50‰ from rock signatures of -90‰ as is observed. The trend of samples in the breccia pipe from -90 to -45‰ thus supports the hypothesis that meteoric water circulation was responsible for hydrogen isotopic alteration and it is reasonable that this occurred during hydrothermal alteration. This is underscored by the excellent correlation between K₂O alteration and δD shown in Figure 12, which suggests that δD exchange took place as alteration occurred.

The very rapid evolution of the hydrogen isotopic alteration (relative to numerical dispersion) makes the models unstable. It has not been possible so far to calculate hydrogen isotopic changes as we did for oxygen.

3.4. Circulation required for chemical alteration

The final test of the physical model is whether it can reproduce the observed chemical/mineralogical alteration summarized in Table IV. Potassium metasomatism, silicification and uranium deposition are all expected for fluids moving down a temperature gradient (Giggenbach, 1988). All these elements have prograde

F4 Borehole Isotopic Analyses

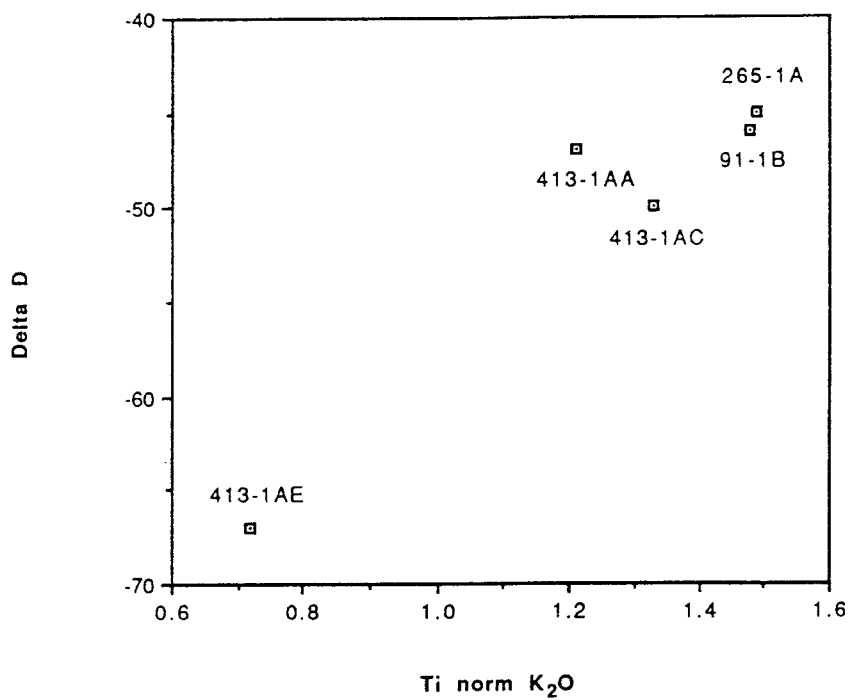


Figure 12. The whole-rock hydrogen alteration of the Poços de Caldas breccia pipe in samples from the hydrothermal hole at the Osamu Utsumi mine shows an excellent correlation with the intensity of chemical alteration.

solubilities. Simple calculations suggest that the observed alteration requires fluid fluxes considerably greater than indicated by the base model, but these fluxes are not unreasonably large.

3.4.1. Silica transport

Because the H_2SiO_3 complex is dominant, silica solubility is dependent only on temperature for waters of slightly alkaline to acid pH at 300°C (300°C fluids in equilibrium with quartz would be ~ 0.01 molal SiO_2). The silica concentration expected for equilibrium with the aluminosilicates (see Table VI) in the breccia at the Osamu Utsumi mine is about half an order of magnitude less, or $\sim 3 \times 10^{-3}$ molal. Taking the lower silica solubility, the 420 moles/cm² of silica addition in the breccia (shown in Table IV) would require 140,000 kg of hydrothermal throughput, or a flux about two orders of magnitude greater than indicated in our base model. This is a minimum estimate because it assumes 100% of the silica dissolved at 300°C is precipitated in the 500 m breccia section.

3.4.2. Potassium, aluminium and sodium transport

The potential of the base physical model of potassium, aluminium, sulfur and fluorine metasomatism and sodium stripping can be evaluated in a fashion similar to that presented above for silica if the composition of the hydrothermal fluid in equilibrium with altered nepheline syenite can be estimated. Because the solubility of the elements in question depends on pH (and in some cases on oxidation state), the evaluation must consider the entire mineralogical buffer system. Because a number of the mineral phases are not stoichiometrically pure end-members and their thermodynamic properties are uncertain, available thermodynamic data can serve only as a guide. Measured solution compositions from hot springs in nepheline syenites would be extremely helpful, but it has been impossible to find any published analyses. Hydrothermal waters in chemical equilibrium with rocks undersaturated in silica would be expected to have a higher pH and, as a result, higher aluminium concentrations than hydrothermal fluids in contact with silica-saturated rocks (Morey and Fournier, 1961). This suggests that aluminium transport is expected in alkaline rocks. The solution compositions should otherwise be similar. Magnesium, for example, should

have a very low solubility at hydrothermal temperatures as it does in siliceous rocks (Fournier, personal communication, 1990).

TABLE V

Dissolution log K values at 300°C used to estimate hydrothermal solution composition at the Osamu Utsumi mine. Dissolution was to the basic elements: Al⁺⁺⁺, Ca⁺⁺, Cl⁻, F⁻, Fe⁺⁺, Fe⁺⁺⁺, H⁺, H₂O, HS⁻, K⁺, Mg⁺⁺, Na⁺ and SiO₂.

Mineral Phase	Column 2	Column 3	Column 4a and b	
	End-member Dissolution log K (300°C)	Dissolution log K Poços stoichiometry	Log K required for basis activity ratios ~ siliceous rocks 300°C 200°C	
Nepheline	3.0	2.8	2.8	5.6
Kalsilite	2.1			
High sanidine	-3.1	-2.8	-2.8	-1.1
High albite	-2.1			
Aegirine	9.6	-2.1	-3	-0.4
Riebeckite	-22.0			
Illite	-5.7	-6.7	-9	-5.7
Max. microcline	-3.5	-3.5	-3.5	-2.2
Kaolinite	-5.3	-5.3	-5.3	-1.6
Fluorite	-13.1	-13.1	-13.1	-10.8
Pyrite	-36.4	-36.4	-36.4	-35.6
14Å-Daphnite	8.7	8.7	8.7	20.4
Hematite	-11.3	-11.3	-11.3	-7.9

Mineralogical issues

Two mineralogical issues must be addressed before it is possible to calculate the chemistry of waters in equilibrium with altered nepheline syenite. The first is the non-end-member stoichiometry of some mineral phases summarized in Table II. Nepheline and high sanidine have been handled by linearly combining the dissolution log K data from the end-member minerals high sanidine (KAlSi₃O₈), high albite (NaAlSi₃O₈) nepheline (NaAlSiO₄) and kalsilite (KAlSiO₄) taken from the EQ3

data-base. For illite, the dissolution log K has been adjusted using an oxide component building-block approach discussed by Chermak and Rimstidt (1989). Because their convention for expressing mineral free energies of formation from the elements differs from Helgeson's and the EQ3 database (in taking the elements up to pressure and temperature when considering the free energy of formation of minerals and aqueous species), the shift in the free energy of formation from end-member illite to the observed Poços stoichiometry was determined using Rimstidt's approach and this change was then applied to the free energy of formation of the end-member illite in the EQ3 database. The dissolution log K at 300°C and 85.93 bars was then calculated for dissolution to the basis species of illite of the Poços stoichiometry by subtracting the illite free energy of formation from the sum of the free energies of formation of the basis species into which it dissolves and dividing by $-2.303 RT$, where R is the gas constant and $T = 573.15^\circ\text{K}$. The results are shown in Table V.

Secondly, the special problem of aegirine augite must be addressed. This pyroxene is extremely unstable in the presence of water at hydrothermal temperatures. It is commonly observed with an alteration rim of riebeckite hornblende (a hydrated form of the original mineral). The authors consider that the outer layers of aegirine augite at Poços ($\text{Na Fe}^{3+}\text{Si}_2\text{O}_6$) were immediately altered to a stoichiometrically equivalent variety of riebeckite ($\text{Na}_{0.5}\text{Fe}_{0.75}^{2+}\text{Fe}_{0.5}^{3+}[\text{Si}_2\text{O}_{5.5}](\text{OH})_{0.5}$) as soon as the augite was exposed to water. This will effectively decrease the dissolution log K of aegirine augite towards the dissolution log K of riebeckite (with the above stoichiometry) as indicated in Table V. A shift of ~ 11 log units, from 9.6 to -2.1, was initially selected. These adjustments to the thermodynamic data are shown in column 3 of Table V.

Solution composition constraints

The change in the dissolution log K of the buffer minerals dictated by the additional requirement that the log activity ratios of the basis species describing the hydrothermal solutions at Poços de Caldas be not too dissimilar from the ratios commonly encountered in hydrothermal systems in siliceous rocks is shown by a comparison of columns 3 and 4a in Table V. The dissolution log Ks of aegirine and illite were first adjusted. These changes gave reasonable results except that the fluxes of HS and F were much too large. To remedy this, the dissolution log Ks of pyrite and fluorite were adjusted as shown. These four changes then give the results presented in Tables VI – VIII.

Table VI shows the log activity ratios of the chemical (basis) species in the hydrothermal solution corresponding to the dissolution log K in Table V. Table VI also compares these log activity ratios to those observed in hydrothermal systems hosted in silica-saturated rocks (“Typical siliceous” column in Table VI). Relatively small changes in dissolution log K cause large changes the activity ratios of the solution.

TABLE VI

Log activity ratio of solutions in equilibrium at 300°C and 85 bars with mineral phases and log K data listed in Table V.

Basis species	Activity ratio	Typical siliceous	Table V col. 3	Table V col. 4a	Poços short basis
Al ⁺⁺⁺	Al ⁺⁺⁺ /(H ⁺) ³	~1.3	-0.12	-0.12	-0.13
Ca ⁺⁺	Ca ⁺⁺ /(H ⁺) ²	~8	-29.6	7.4	
F ⁻	FH ⁺		8.3	-10.3	
Fe ⁺⁺	Fe ⁺⁺ /(H ⁺) ²	~3.5	3.3	3.3	
Fe ⁺⁺⁺	Fe ⁺⁺⁺ /(H ⁺) ²	~-6	-5.7	-5.7	-3.9
HS ⁻	HS ⁻ (H ⁺)		-10.9	-10.9	
K ⁺	K ⁺ /H ⁺	~4	4.2	4.2	4.2
Mg ⁺⁺	Mg ⁺⁺ /H ⁺) ²	~5	49.0	3.0	
Na ⁺	Na ⁺ /H ⁺	~5	5.9	5.9	5.9
SiO ₂	SiO ₂	-2.0	-2.5	-2.5	

Predicted metasomatism

Table VII shows the moles per cm² of Na, K, Al and SiO₂ added (positive) or removed (negative) by 100,000 kg of hydrothermal solution circulating from 300 to 200°C in equilibrium with nepheline, high sanidine, hydrated aegirine augite, maximum microcline, illite, kaolinite, fluorite, pyrite, 14Å-daphnite and hematite.

Table VII shows that the mineral buffer and the changes in pore-water composition it causes as temperature falls from 300 to 200°C, can produce the metasomatic alteration observed in the Poços de Caldas breccia provided ~10⁵ kg of hydrothermal solution circulate through every square centimeter plan cross-section of the pipe. In the calculations, pH was determined by charge balance from the log activity ratios in Table VI. The contribution of all the complexes in the EQ3 database to the total concentration of the basis species in the hydrothermal solution was calculated using a program equivalent to EQ3. The metasomatic additions of the basis species to the breccia pipe between the 300° and 200°C horizons (roughly 500 m apart in a boiling

TABLE VII

Metasomatic additions in moles to the host rock that would be produced if 10^5 kg/cm² of hydrothermal solution in equilibrium with mineral buffers described in the text is circulated past 300° and 200°C horizons in the pipe. The fluxes should be compared to those required to alter a 500 m section of the Poços de Caldas breccia pipe at the Osamu Utsumi mine listed in Table IV. This comparison is facilitated by the last column which gives the petrologically inferred metasomatic changes of Table V normalized to 162 moles/cm² of SiO₂ addition. Calculations are made for both boiling and non-boiling systems. The maximum temperature in the boiling calculations was 350°C. The depth interval between 300° and 200°C in the boiling system lies between 667 to 140 m depth, assuming the pressure gradient is cold water hydrostatic as it is in most natural systems. Boiling affects the metasomatic fluxes because it changes solution salinity and pH, but the effects are not too great. Precipitation is reduced in the boiling systems because part of the water-mass flux is carried by the vapor phase, which transports no non-volatile species.

Cl _{tot} (ppm):	Buffer: Ne-HSan-HydAegAug-III-MMicr-Kaol-Fluo-Py-Daph-Hem								Inferred from petrol. observ.
	1000		5000		10,000		42,000		
	no boil	boil	no boil	boil	no boil	boil	no boil	boil	
Na	-2920	-1190	-1510	-586	-1110	-576	-1520	-1310	-112
K	54	51	191	187	350	341	1230	1200	56
Al	691	473	213	144	131	90	59	42	56
SiO ₂	167	157	175	162	178	163	181	164	162

system) were then determined by subtracting the total basis species concentrations in equilibrium with the rock buffer minerals at 300°C (the inflow temperature) and 200°C (the outflow temperature). The metasomatic additions have the units moles per cm² plan cross-section of the pipe.

The stripping of sodium and addition of silica, aluminium and potassium, calculated in Table VII from the thermodynamic data in Table V (col. 4) and simple down-temperature flow, is comparable with that observed in the pipe. The intensity of Na depletion is greatest at both low salinities (where pH is highest) and high salinities (where there is more Cl⁻ to charge balance Na⁺). Potassium enrichment increases with salinity, while Al metasomatism decreases (due to changes in pH). Silica metasomatism is independent of salinity. The approximately equal additions of K and Al observed in the Poços de Caldas breccia are most compatible with the cooling of a ~1 wt.% (5,000 ppm Cl⁻) solution. This is less than the 7% salinity indicated by fluid inclusions in fluorite.

It is clear from Tables VII and IV that about 10^5 kg of hydrothermal solution per cm² of breccia is required to produce the alteration observed. This is required not only by the silica additions, where the thermodynamic data are well-known and uncomplicated

by mineral interactions, but also for all the major elements (K, Na, Al). A fluid flux of 10^5 kg/cm² is a two to three order-of-magnitude increase in flow through the pipe over that indicated in the base model (Figs. 6–9).

Predicted petrologic alteration

The metasomatic fluxes to the rock indicated in Table VII can be combined with the stoichiometry of the buffer minerals to determine the petrologic changes that correspond to these fluxes. Table VIII shows the calculated petrologic alteration of the Poços de Caldas breccia. The observed 60 wt.% destruction of high sanidine, 10 wt.% destruction of aegirine and 60 and 23 wt.% deposition of maximum microcline and illite (Table II) are well-simulated for solutions around 10,000 ppm Cl⁻. The calculated mineralogical changes show, however, destruction of kaolinite and precipitation of nepheline, which is the opposite of that observed. As discussed below, the mineralogical changes are extremely sensitive to even very small changes in thermodynamic data or mineral stoichiometry. However, it is certain that thermodynamically compatible dissolution log K and reasonable mineral stoichiometries can be found that will produce calculated petrologic changes fully compatible with those observed. Identifying the right parameters is not

TABLE VIII

Major changes in mineralogy (expressed in wt.%) as predicted by the alteration model described in the text. Dissolved (or converted) and new minerals separately sum to 100 wt.%. The observed alteration is from Table II. The calculated alteration is given for the throughput of 10^5 kg of hydrothermal solution between the 300° and 200°C planes.

	observ.	ppm Cl ⁻			
		1000	5000	10,000	42,000
High sanidine	-60	-23	-55	-63	-85
Nepheline	-30	15	1.5	8	2
Aegirine	-10	-21	-14	-12	-5
Kaolinite	14	-43	-22	-20	-9
Illite	23	74	49	39	15
Max. microcl.	60	-81	33	47	80

straight-forward and possibly not warranted for bulk estimates of petrologic alteration over a broad temperature (and space) interval. Laboratory experiments could best determine the required parameters.

Sensitivity

Before discussing laboratory experiments, a further aspect of the mineralogical alteration should be noted that has important implications for the kinds of approaches to rock alteration that will be most effective. The studies reported here show that mineralogical alteration is extremely sensitive to small changes in thermodynamic data. This is illustrated in Table IX which shows that changing the dissolution log K of aegirine by even 0.01 log units completely changes the nature of the predicted alteration. The mineralogy is much more sensitive than the metasomatic flux to slight changes in the dissolution log K, because all components of the rock flux must be

TABLE IX

The sensitivity of mineralogical alteration to slight changes in dissolution log K data. The "Base" case is the same as in Table VII for 5000 ppm Cl⁻ in a boiling system. The calculation in the "Fluorite change" column is identical to the base case, except that the dissolution log K for fluorine is -13.1 rather than -13.2. The "Aegirine change" column is identical to the base case, except that the dissolution log K for aegirine has been changed from -3.0 to -2.99. Changes in other mineral dissolution log K show less sensitivity.

	Base	Fluorite change	Aegirine change
Major mineral			
High sanidine	-55	-20	-22
Nepheline	1.5	18	-20
Aegirine	-14	-22	14
Kaolinite	-22	-46	36
Illite	49	77	-49
Max. microcl.	33	-9	39
Major total basis flux in moles/cm²			
Na ⁺	-586	-520	-630
K ⁺	187	188	186
Al ⁺⁺⁺	144	202	108
SiO ₂	162	162	162

accommodated in rock minerals. Thus, small changes in metasomatic flux have a disproportionate effect on the mineralogy. A good part of the sensitivity of the calculated mineralogical alteration to thermodynamic and stoichiometric data is due to the rigorous assumption of local equilibrium in the models used in this study. Kinetics will reduce the sensitivity, but not eliminate it. Substantial sensitivity will remain.

It is important to calculate mineralogical alteration accurately because alteration minerals may provide structural homes for radionuclides and thus affect their migration.

Calibration experiments

Given the inevitable uncertainties in thermodynamic estimates and the non-end-member stoichiometries of the mineral phases (which may change with time in a chemically evolving natural system or repository), it may be unrealistic to expect to calculate mineralogical alteration directly from thermodynamic data. A better way to proceed would be to calibrate a thermodynamic model such as the one developed here through laboratory experiments. In principle, it should be possible to invert the chemical composition of solutions equilibrated in the laboratory with altered Poços de Caldas nepheline syenite to give dissolution log K values for the buffer minerals required to simulate the solution chemistry. If this were done at both 200° and 300°C, for example, the metasomatic fluxes of Table IV could be directly tested. Having confidence in the calibrated dissolution log K values, mineral stoichiometries could be adjusted within reasonable limits so that models simulated both the correct metasomatic fluxes (to the rock) and the alteration mineralogy. Alteration models could be further tested by column experiments such as those described in section 4.

3.5. Increasing hydrothermal circulation through the breccia at the Osamu Utsumi mine

Rough heat balance calculations show that it is quite feasible to increase the hydrothermal flux through the breccia by the 2 1/2 orders of magnitude required by the chemical alteration data, but that much greater increases are implausible. An absolute upper limit is a 3.5 order-of-magnitude increase over the base model. The contribution of magmatic water cannot be significant.

The main ways to increase the hydrothermal flux through the breccia are: (1) putting the problem in a three dimensional rather than two-dimensional context and (2) increasing the depth of hydrothermal water circulation (or the depth extent of the magma chamber from which heat is being extracted).

In the model calculations, the volumetric heat capacity of nepheline syenite was taken to be $0.54 \text{ Cal/cm}^3\text{-}^\circ\text{K}$. This was augmented by 30% in the intrusion to account for latent heat of crystallization. Thus the intrusive (2.12 km^2 in cross-sectional area for half the intrusion) could supply $8.9 \times 10^{12} \text{ J}$ in cooling from 700° to 100°C . If the heat were carried off by waters that were heated to 350°C after interacting with the intrusion, the intrusion could circulate about $2.55 \times 10^{10} \text{ g}$ of hydrothermal solution, or a volume, at 1 g/cc water density, about 1.2 times bigger than the volume of the intrusion. If this hydrothermal solution were vented through dyke-like breccia pipes 500 m wide on each side of the dyke-like (e.g. two-dimensional) intrusion, the average mass flux through each pipe would be $\sim 510 \text{ kg/cm}^2$. This is satisfyingly close to the average that can be inferred from Figure 9, which indicates that, during the stages of cooling when portions of the intrusion are still hotter than 300°C , most of the heat is vented through the pipe. A very water-rich intrusion (Dudas, 1983) might contain 10 vol.% volatiles. Thus, the magmatic volatiles are less than 20% of meteoric water circulation and cannot significantly increase the amount of hydrothermal solution circulated by the intrusion. For further discussion of this analysis approach see Cathles (1983).

In three dimensions, a slightly larger intrusion 6 km in diameter lying 3 km below the surface and extending to 10 km depth could reasonably feed 3 breccia pipes 500 m in diameter. Making the same calculation shows that the hydrothermal flux through each pipe should be $4 \times 10^4 \text{ kg/cm}^2$, or 1.9 orders of magnitude greater than the base case. This can be increased by 0.3 log units if flow is focussed in 50% of the pipe, by 0.25 log units if the pipe were 4 km in radius rather than 3 and by 0.15 log units if the intrusion extended to 13 km rather than 10 . Cumulatively, these reasonable changes could increase the hydrothermal flux through each breccia pipe by 2.6 orders of magnitude over the base case.

A limit to the increase in hydrothermal flux is provided by assuming an intrusive heat source the diameter of the Poços de Caldas caldera (30 km) extending through a 43 km thick crust (e.g. 40 km in depth extent, 3 km below the surface). If this intrusive heat source fed 500 m diameter breccia pipes from 5 km deep centers, the hydrothermal flux through each pipe would be $1.9 \times 10^6 \text{ kg/cm}^2$, an increase of 3.6 orders of magnitude over the base model. This can be considered an upper boundary on a

geologically plausible hydrothermal flux through a breccia pipe such as that at the Osamu Utsumi mine.

It can therefore be concluded that the flux suggested by the chemical alteration of the breccia pipe at the Osamu Utsumi mine is quite reasonable, but indicates a larger intrusion with greater depth extent than in the base model (Figs. 4 and 6) and effective flow concentration through the pipe. The 5 orders of magnitude increase in hydrothermal throughput required by recent estimates of uranium solubility and the uranium mineralization of the pipe is not geologically reasonable. Ways must apparently be found to increase the uranium solubility under geological conditions by at least 1.5 orders of magnitude if natural examples of mineralization such as Osamu Utsumi are to be understood. In addition, as previously discussed, if the solubility of uranium is not temperature-sensitive, a precipitation mechanism must be identified.

3.6. A circulation model compatible with all chemical data

It was assumed with the chemical analyses that the temperature dropped about 100°C over a 520 m section of the pipe. The best way to achieve this kind of temperature drop is through fluid boiling. For the calculated solution chemistry, boiling does not significantly affect the rate or character of metasomatic alteration (since all the elements considered in the mass balance calculations are left behind in the liquid phase). Boiling and non-boiling metasomatic fluxes are compared in Table VII. A temperature drop from 300°C to 200°C will occur over a 520 m depth interval with its top 140 m below the groundwater table.

In summary, then, the simplest physical model that will account for all the petrologic observations (including the indications of boiling and salinity in fluid inclusions) is that an intrusion 6 km in diameter and extending 10 km in depth circulated hydrothermal fluid through ~3 breccia pipes as it cooled by convective interaction with meteoric water. Uranium, K, SiO₂, Ca and F were added to the nepheline syenite fragments in the breccia pipes and Na stripped primarily where the solutions dropped in temperature due to boiling. A 500-m-thick section of each pipe could be altered as observed at Osamu Utsumi where the hydrothermal fluids dropped from 300°C to 200°C by boiling. The throughput of hydrothermal solution required to produce the observed uranium mineralization and chemical rock alteration is ~10⁵ kg hydrothermal solution per cm² cross-sectional area (in plan view) of the breccia pipe.

Because the hydrothermal fluid circulation was increased by 2 1/2 orders of magnitude by increasing the mass of the intrusion heat source, the isotopic evolution from the recharge zones will not significantly change from the base model already discussed. For example, the near-surface meteoric alteration in Figure 11 will penetrate to greater depths, but only in proportion to the increased depth extent of the intrusion. The oxygen isotopic alteration will thus be controlled by temperature gradient phenomena associated with hydrothermal interaction with the heat source and hydrogen isotopic alteration will be controlled by the δD of the meteoric water influx to the system. In other words, all aspects of the chemical and isotopic alteration are compatible with the physical model sketched above, which is a relatively minor modification of our base model. It should, however, be noted that the effects of boiling on the isotopic alteration have not been taken into account and the above statement assumes boiling will not significantly affect the whole-rock isotopic alteration.

4. Chemical experiments to test alteration models

Some preliminary experiments have been carried out in a flow-through temperature gradient apparatus to test the general validity of the chemical model developed above. The apparatus will be fully described in Newcomb and Cathles (1990; in preparation). Water was passed through a sample of unaltered Poços de Caldas nepheline syenite crushed to <88 but >53 microns. The crushed rock material was placed in a 120 cm long, thick-walled 316 stainless steel tube with 1 cm² inner diameter. The tube was pressurized to 238 bars. The central part of the tube was heated to 350°C and water passed through the tube at 5 microliters per minute for 200 hours. The run was terminated by a failure in the thermal control. As a result, the tube was subjected to temperatures of 500°C for about 24 hours. Because the alteration is believed to be tied to solution throughput, this high-temperature episode is not expected to significantly affect the metasomatic alteration observed in the nepheline syenite.

The altered nepheline syenite was examined after the run with a scanning electron microscope with EDAX capability. The nepheline syenite showed almost no Na at any location and was almost entirely Al and Si. The surface is typically densely covered by rounded crystals as if the face were being dissolved along particular crystallographic orientation. (Fig. 13). Sodium appears to be leached regardless of whether the fluid is flowing up or down the temperature gradient. Thus, as observed in the Osamu Utsumi

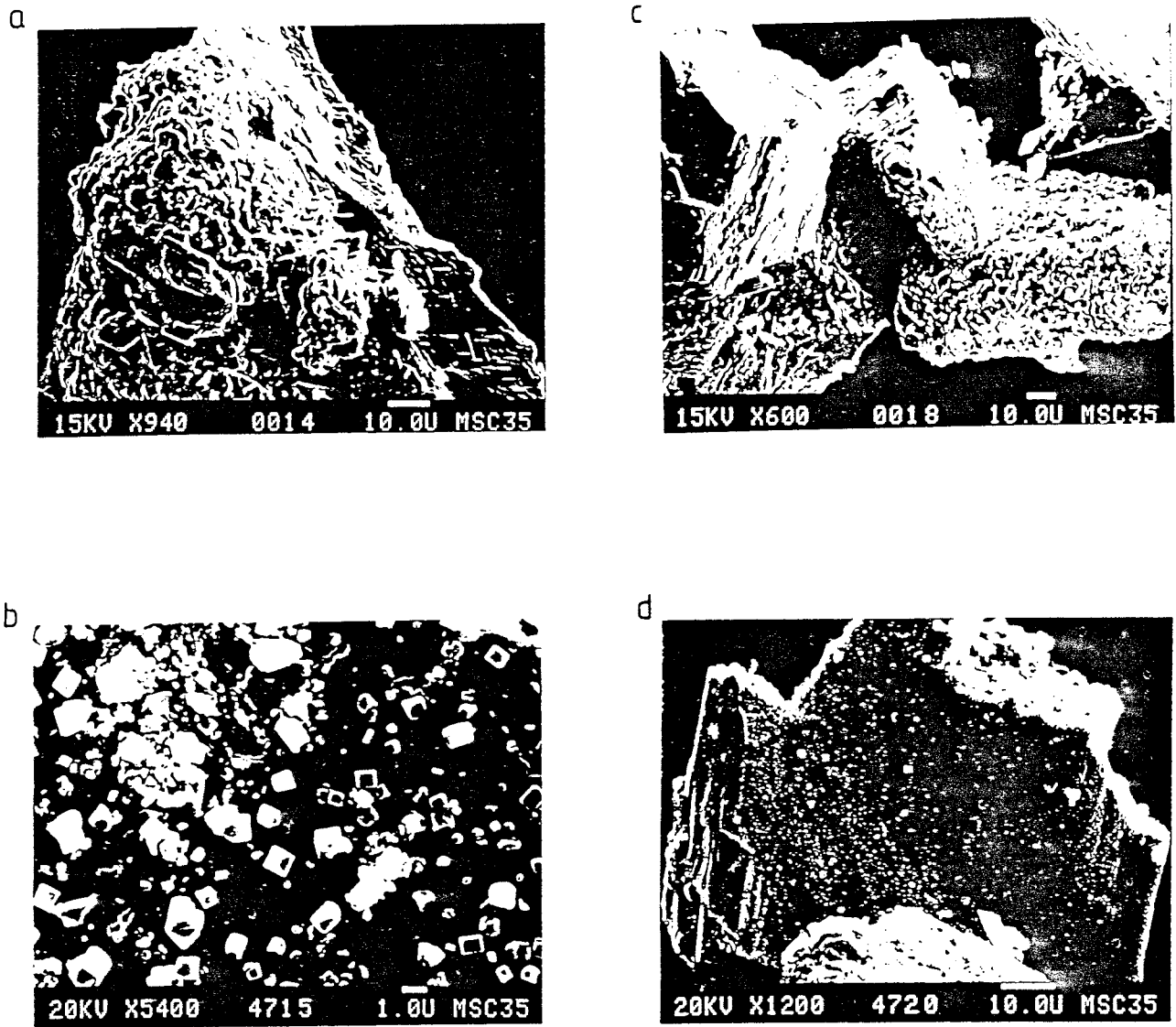


Figure 13. Series of figures showing the alteration of nepheline syenite, sanidine and aegirine augite in the temperature gradient flow experiment described in the text. (a) Nepheline syenite dissolving along crystallographic orientations in a portion of the tube where fluid is flowing up-temperature at $T \sim 350^\circ\text{C}$. (b) Sanidine with etch pits in the down-temperature part of the column covered with K-feldspar cubes precipitated on the surface during the experiment. (c) Unaltered sanidine (left) next to altered nepheline (right) in the up-temperature part of the tube. (d) Aegirine augite in the down-temperature portion of the tube covered with a fine honeycomb of small crystals.

breccia samples, Na was leached very rapidly from the surface layer of the nepheline syenite and removed by the hydrothermal solution.

The sanidine was pitted and overgrown with euhedral rhombs of K-feldspar on the down-temperature side of the column (Fig. 13b). On the up-temperature side, K-feldspar appears unaltered (Fig. 13c on left; note altered nepheline grain to right). Thus sanidine is destroyed and replaced by maximum microcline in areas where solutions are flowing down a temperature gradient. This is compatible with the theoretical model and petrologic observations in the Osamu Utsumi breccia pipe.

Aegirine augite also does not appear to be altered on the up-temperature side of the column, but is altered on the down-temperature side. On the down-temperature gradient side, one face of the aegirine augite is typically smooth and the other face completely covered by small crystals which consist of Ca, Al, Si and Fe (Fig. 13d). These small crystals could reflect the alteration to a riebeckite-type phase, as hypothesized in the chemical discussion above. However, this would not explain the apparent lack of reactivity on the up-gradient side, which should occur if the aegirine is as thermodynamically unstable as believed.

In summary, the column results appear to support the chemical model presented above in most aspects. However, the results described should be considered preliminary.

5. Prediction of the near-field uranium transport and alteration at a hypothetical high-level waste repository

Design parameters for a hypothetical underground high-level radioactive waste repository were selected from the U.S. DOE (1988). In this design, a hypothetical repository of 70 thousand metric tonnes uranium would require 18 burial panels. Each panel would be 450 x 900 m in plan dimension excavated at a depth of 200 to 500 m. In the floor of each panel, vertical waste canisters with 0.7 m diameter would be emplaced at 5 m spacing. Each canister would be 3 m long. The 18 panels would cover an area 3 km x 3 km. The heat generation in the paneled area would initially be 0.014 kilowatts per m². The rate of radioactive heat generation would decay with time in a fashion that can be described by the following equation:

$$\frac{\text{Heat Generation}}{\text{Initial Heat Generation}} = 0.5 e^{-t/0.2} + 0.5 e^{-t/3}$$

In this equation t is time in thousands of years.

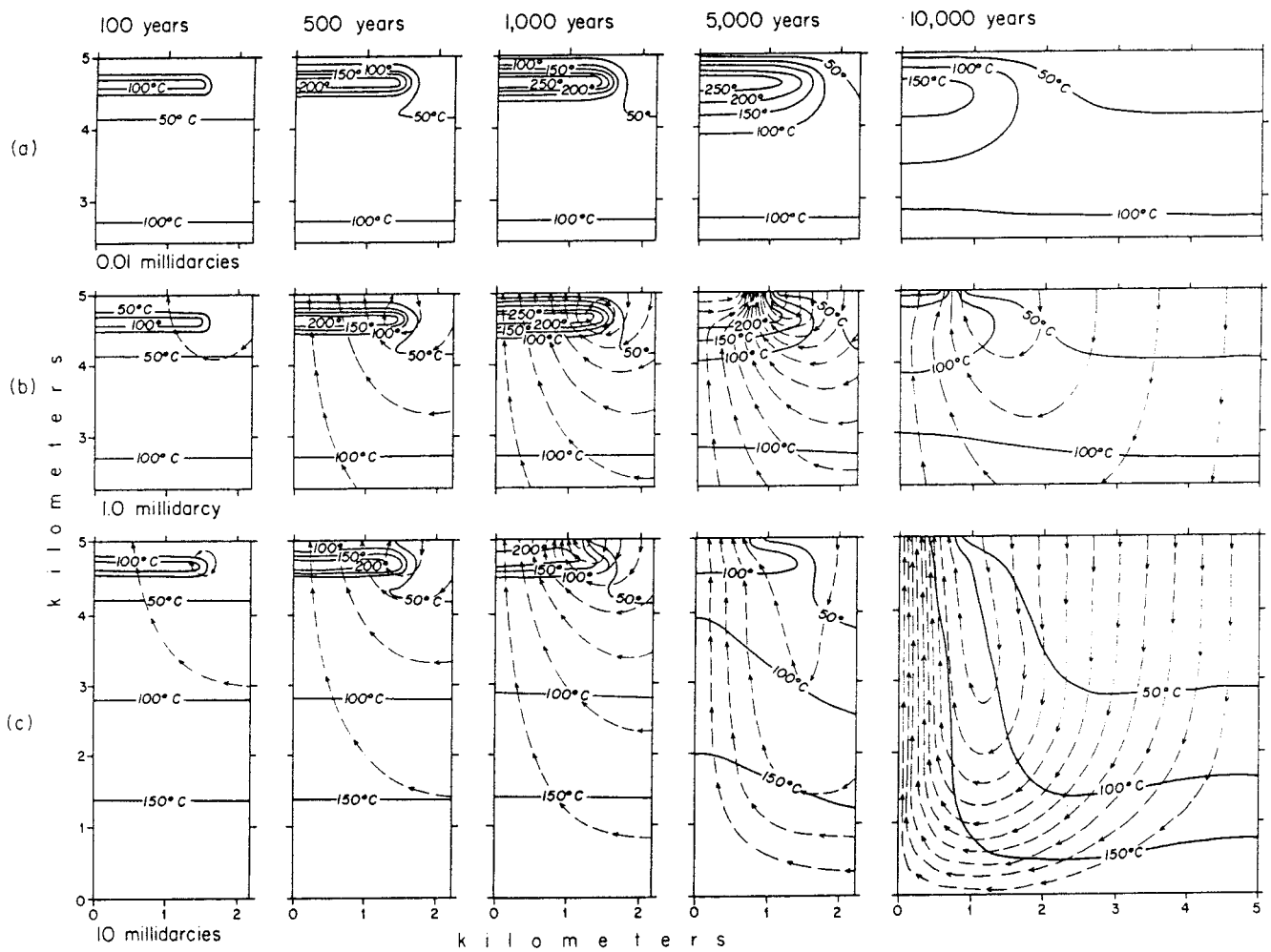


Figure 14. Calculated temperature and fluid convection around the 70 kt high-level nuclear waste repository described in the text. (a) Host is essentially impermeable; repository reaches temperatures limited only by conduction. (b) Host has permeability of 1 millidarcy, similar to environment at Poços de Caldas. Convection is induced to at least 5 km depth and temperature of repository at any time is reduced. (c) Host has permeability of 10 millidarcies; convection and cooling of the repository are greater.

The fluid circulation such a waste repository would produce over its 10,000 year statutory life can be calculated using the same techniques used to calculate the flow that led to the mineralization of the Poços de Caldas breccia pipe. In the calculations, a heated layer (200 m thick) representing the repository is assumed to be at a depth of 250 to 450 m. The heat generation per unit area as given in the above formula was converted to a uniform volumetric heat generation rate throughout the 200-m-thick zone. As in the Poços de Caldas case, no boiling was allowed in the fluid flow calculations, although in the real case boiling will certainly occur. The environment of the repository is assumed to be water-saturated. The amount of fluid circulation and temperature depend on the host permeability. The calculations are carried out assuming a uniform permeability in a 10 km wide, 5 km deep domain around and including the repository. The thermal conductivity of the computational domain was 4.2×10^{-3} cal/cm-sec-°C.

The results are shown in Figure 14. If the permeability is very low (0.01 millidarcies; Fig. 14a), the repository heats up to a maximum temperature of 327°C 2,500 years after burial and then cools as the radioactive material decays and loses heat generation capacity. If the permeability of the host and repository is 1 millidarcy, substantial convection occurs to ~5 km depth, as shown in Figure 14b. The repository reaches a maximum temperature of 318°C 2,400 years after waste emplacement. Finally, if the permeability of the repository and its setting is 10 millidarcies, more convection occurs through the repository (Fig. 14c). The waste reaches a maximum temperature of 245°C 900 years after emplacement.

The amount of fluid circulated through the hypothetical repository depends on the permeability. For 10 darcy, permeability-free (Rayleigh-Bernard) convection is substantial soon after radiogenic heating has decayed and is focussed on the repository. No topography-driven fluid flow is considered, which could change the pattern of convection substantially. Figure 15 shows the maximum cumulative fluid flux above the hypothetical repository for the 1 and 10 millidarcy cases. Figure 15 also indicates the points on the cumulative fluid flux curves where the repository first reaches 200 and (if applicable) 300°C, and where the repository again cools through these temperatures. The repository system will circulate at most about 100 kg/cm² of hydrothermal solution that has interacted with rock hotter than 200°C. Most of the greater mass flux in the 10 millidarcy case occurs after the repository has cooled below 200°C and is associated with natural Rayleigh-Bernard convection driven by the normal heat flux from the earth's interior. This is evident in the pattern of cumulative fluid flux shown in Figure 16.

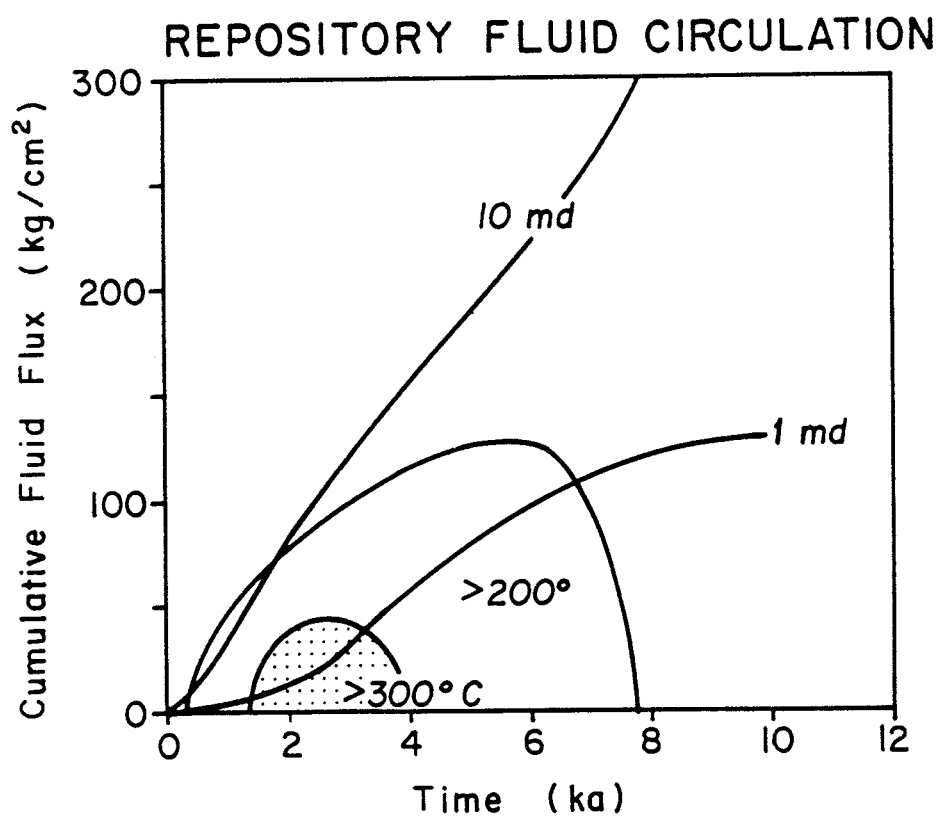


Figure 15. Cumulative fluid flux for the 1 and 10 millidarcy cases as shown in Figure 14. Points along curves at which a hypothetical repository first exceeds 200° and 300°C, and the points at which the maximum temperature again drops below these values, are indicated and contoured. The time-cumulative flux domain where temperatures are greater than 300°C are stippled. This figure shows that less than ~100 kg/cm² of fluids hotter than 200°C will circulate through the hypothetical repository.

REPOSITORY CUMULATIVE CIRCULATION AT 10,000 YEARS

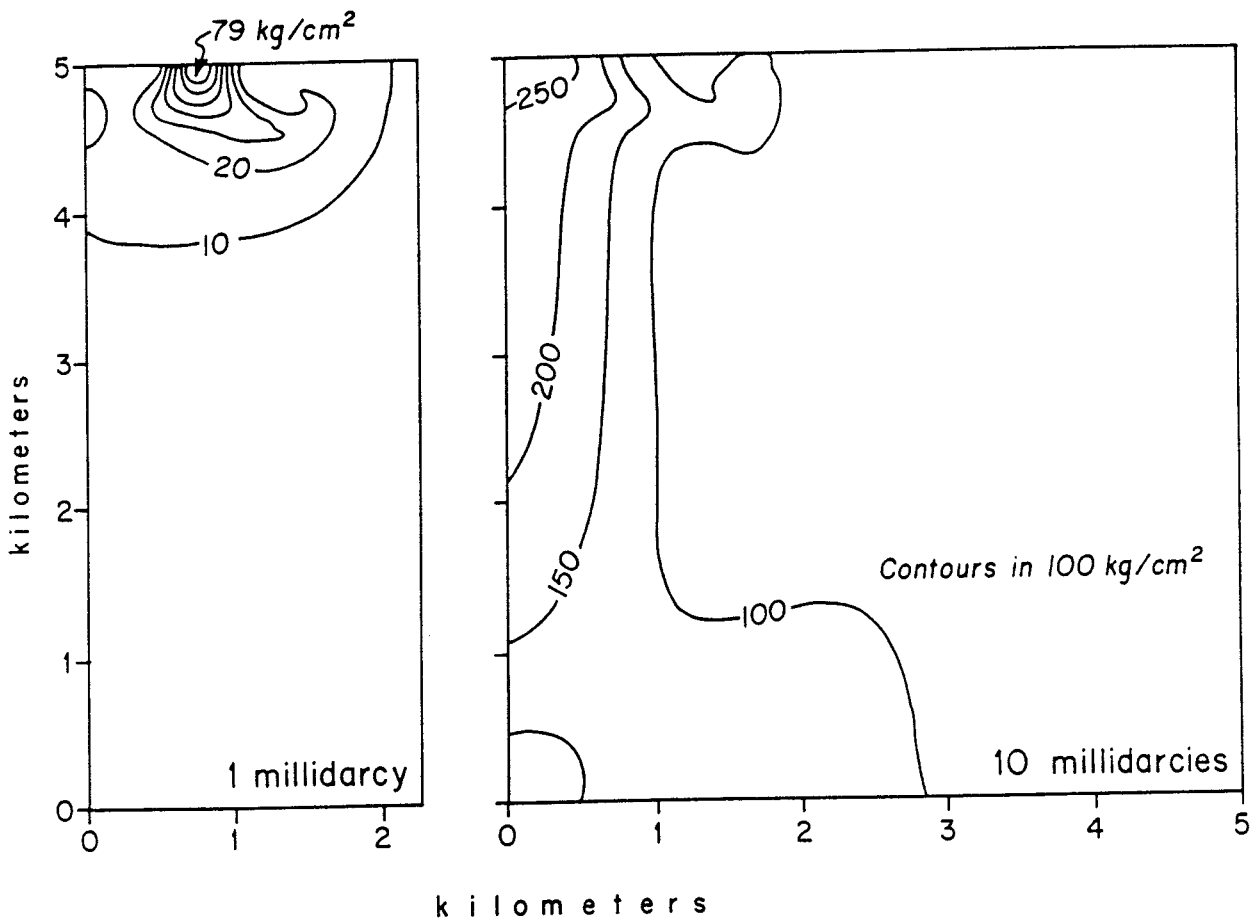


Figure 16. Cumulative fluid circulation through the hypothetical repository after 10,000 years. Here, as in previous figures, the repository is assumed to have exactly the same permeability as the host into which it is emplaced (i.e. it is assumed that no steps are taken to inhibit flow through the repository). The large circulation in the 10 millidarcy case is mostly due to free Raleigh-Bernard convection occurring in the earth's normal thermal gradient at these high permeabilities. The free convective flow is centered on the hypothetical repository by the radiogenic heating and continues indefinitely, long after the waste has decayed.

Figures 14–16 show that fluid flow in and around a typical high-level waste repository may be strikingly similar to that in the Poços de Caldas analogue. The depth of fluid circulation, the maximum temperatures reached, the thickness of the zone where temperatures will drop from ~ 300 to $< 200^\circ\text{C}$ and the probability of fluid boiling are all similar. The main difference is that the Poços de Caldas breccia focussed flow in a dramatic fashion, so that the mineralized parts of that system experienced fluid fluxes of $\sim 10^5$ kg/cm² rather than $\sim 10^2$ kg/cm² calculated for a hypothetical repository emplaced in a region with permeability more than 1 millidarcy. Since chemical transport and alteration depend, all other factors being equal, only on the mass of fluid circulated, the three order-of-magnitude difference in the mass of fluid circulated indicates that the alteration and uranium enrichment in and above the hypothetical repository will be about 0.1% of that observed in the breccia pipe at the Osamu Utsumi mine. That is, uranium enrichment in 10,000 years above the hypothetical repository (assuming full waste access and saturation of uranium in solution) will be on average about 0.05 ppm (vs. 50 ppm in the Poços de Caldas breccia). The total mass added by alteration will be on average about 0.3 wt.% (vs. 30 wt.%). The K₂O enrichment (if the host is nepheline syenite) will be on average about 4×10^{-3} wt.% (vs. the 4 wt.% in Table VI). As in the analogue case, the hypothetical repository calculations emphasize the importance of knowing, or at least carefully estimating, the permeability of the whole system (e.g. permeabilities to ~ 5 km depth, etc). This is particularly important, as Figure 16 shows, if the permeability of the system is greater than a few millidarcies.

6. Conclusions and recommendations for future work

In summary, a careful examination of a natural example of radionuclide transport and concentration under hydrothermal conditions has contributed to our understanding of both the ore-forming process and the likely alteration and radionuclide transport at a high-level waste repository on a 10,000 year timescale. Despite a lack of knowledge of much of the natural system, it can reasonably be ascertained that the intense alteration observed in the Poços de Caldas breccia pipe required a cumulative fluid flux of $\sim 10^5$ kg/cm². Fluids probably circulated to ~ 10 km depth through rock that had at least 1 millidarcy permeability. Uranium deposition occurred when the upwelling fluids, focussed in a few high-permeability breccia pipes, boiled.

The same procedures applied here to the mineralization of the Osamu Utsumi mine have been applied to a hypothetical waste repository. The temperatures, system scale and mechanisms of alteration and precipitation (steep temperature gradient maintained in part by boiling) were found to be remarkably similar between the natural analogue and the repository. The main difference is that about three orders of magnitude less hydrothermal ($T > 200^{\circ}\text{C}$) fluid is expected to pass through the hypothetical repository in even the worst scenario (completely open to fluid incursion, permeability equal to that in the surrounding rock). As a result, the average alteration and radionuclide transport will be at worst less than 0.1% of that encountered in primary (hypothermal) alteration in the breccia pipe at the Osamu Utsumi mine.

The mineralogy of the calculated alteration is extremely sensitive to the thermodynamic data characterizing the reacting minerals, so much so that it may only be possible to obtain thermodynamic data accurate enough to predict alteration by inverting petrologic observations of laboratory or field alteration, as has been done in a crude fashion in this present study. In other words, it may be advantageous to use the framework and starting estimates of available thermodynamic data, but to refine that data for each repository or host rock type.

A set of laboratory experiments to determine the solution composition at different temperatures, pressures and salinities could be directly inverted to give thermodynamic data for the mineral phases known to be involved in the reactions. The data could then be used to calculate the alteration caused by evolution of the physical convective system. It is recommended that this approach be pursued and in particular that such experiments be carried out.

7. References

- Appleyard, E.C., 1980. Mass balance computations in metasomatism: metagabbro/nepheline syenite pegmatite interactions in northern Norway, *Contrib. Mineral. Petrol.*, 73, 131-144.
- Babcock, R.S., 1973. Computational models of metasomatic processes. *Lithos*, 6, 279-290.
- Cathles, L.M., 1977. An analysis of the cooling of intrusives by ground water convection which includes boiling. *Econ. Geol.*, 72, 804-826.

- Cathles, L.M., 1983. An analysis of the hydrothermal system responsible for massive sulfide deposition in the Hokuroku Basin of Japan. *Econ. Geol., Monogr. 5*, 439-487.
- Cathles, L.M., 1990. The importance of vein selvaging in controlling the intensity and character of hydrothermal alteration in the deeper (>1km deep) portions of hydrothermal systems. *Econ. Geol.* (In preparation)
- Chermak, J.A., and Rimstidt, J.D., 1989. Estimating the thermodynamic properties ΔG_f° and ΔH_f° of silicate minerals at 298°K from the sum of polyhedral contributions. *Am. Mineral.*, 74, 1023-1031.
- Cole, D.R., Mottl, M.J. and Ohmoto, H., 1987. Isotopic exchange in mineral-fluid systems. II: Oxygen and hydrogen isotopic investigation of the experimental basalt – seawater system. *Geochim. Cosmochim. Acta*, 51, 1523-1538.
- Dudas, F.O., 1983. The effect of volatile content on the vassiculation of submarine basalts. *Econ. Geol., Monogr. 5*, 134-141.
- Friedman, I. and O'Neil, J.R., 1977. Compilation of stable isotope fractionation factors of geochemical interest. In: M. Fleischer (Editor). Data of Geochemistry, 6th Edition. *U.S. Geol. Surv. Prof. Pap.*, 440-kk.
- Giggenbach, W.F., 1988. Geothermal solute equilibria. Derivation of Na-K-Mg-Ca geoindicators. *Geochim. Cosmochim. Acta*, 52, 2749-2763.
- Gresens, R.L., 1967. Composition-volume relationships of metasomatism. *Chem. Geol.*, 2, 47-65.
- Kertes, A.S., and Guillaumont, R., 1985. Solubility of UO_2 . A comparative review. *Nucl. Chem. Waste Manag.*, 5, 215-219.
- Morey, G.W., and Fournier, R.O., 1961. The decomposition of microcline albite and nepheline in hot water. *Amer. Mineral.*, 46, 688-699.
- Newcomb, W., and Cathles, L.M., 1990. Alteration of rocks by flow through a temperature gradient. *Econ. Geol.* (In preparation.)
- Parks, G.A., and Pohl, D.C., 1988. Hydrothermal solubility of uraninite. *Geochim. Cosmochim. Acta*, 52, 863-875.
- Sheppard, S.M.F., 1986. Characterization and isotopic variations in natural waters. In: Stable Isotopes in High Temperature Geological Processes. *Min. Soc. Amer. Revs. Min.*, 16, 165-183.

- Taylor, H.P.O., 1979. Oxygen and hydrogen isotopic relationships in hydrothermal mineral deposits. In: H.L. Barnes (Editor). *Geochemistry of Hydrothermal Ore Deposits*. *John Wiley*, New York, 236-277.
- U.S. Department of Energy, 1988. Site characterization plan, Yucca Mountain Site. In: Nevada Research and Development Area, Nevada. Vol. III, Part A (DOE/RW-0199).

List of SKB reports

Annual Reports

1977-78

TR 121

KBS Technical Reports 1 – 120

Summaries

Stockholm, May 1979

1979

TR 79-28

The KBS Annual Report 1979

KBS Technical Reports 79-01 – 79-27

Summaries

Stockholm, March 1980

1980

TR 80-26

The KBS Annual Report 1980

KBS Technical Reports 80-01 – 80-25

Summaries

Stockholm, March 1981

1981

TR 81-17

The KBS Annual Report 1981

KBS Technical Reports 81-01 – 81-16

Summaries

Stockholm, April 1982

1982

TR 82-28

The KBS Annual Report 1982

KBS Technical Reports 82-01 – 82-27

Summaries

Stockholm, July 1983

1983

TR 83-77

The KBS Annual Report 1983

KBS Technical Reports 83-01 – 83-76

Summaries

Stockholm, June 1984

1984

TR 85-01

Annual Research and Development Report 1984

Including Summaries of Technical Reports Issued during 1984. (Technical Reports 84-01 – 84-19)

Stockholm, June 1985

1985

TR 85-20

Annual Research and Development Report 1985

Including Summaries of Technical Reports Issued during 1985. (Technical Reports 85-01 – 85-19)

Stockholm, May 1986

1986

TR 86-31

SKB Annual Report 1986

Including Summaries of Technical Reports Issued during 1986

Stockholm, May 1987

1987

TR 87-33

SKB Annual Report 1987

Including Summaries of Technical Reports Issued during 1987

Stockholm, May 1988

1988

TR 88-32

SKB Annual Report 1988

Including Summaries of Technical Reports Issued during 1988

Stockholm, May 1989

1989

TR 89-40

SKB Annual Report 1989

Including Summaries of Technical Reports Issued during 1989

Stockholm, May 1990

Technical Reports

List of SKB Technical Reports 1990

TR 90-01

FARF31 –

A far field radionuclide migration code for use with the PROPER package

Sven Norman¹, Nils Kjellbert²

¹Starprog AB

²SKB AB

January 1990

TR 90-02

Source terms, isolation and radiological consequences of carbon-14 waste in the Swedish SFR repository

Rolf Hesböl, Ignasi Puigdomenech, Sverker Evans
Studsvik Nuclear

January 1990

TR 90-03

Uncertainties in repository performance from spatial variability of hydraulic conductivities – Statistical estimation and stochastic simulation using PROPER

Lars Lovius¹, Sven Norman¹, Nils Kjellbert²

¹Starprog AB

²SKB AB

February 1990

TR 90-04

Examination of the surface deposit on an irradiated PWR fuel specimen subjected to corrosion in deionized water

R. S. Forsyth, U-B. Eklund, O. Mattsson, D. Schrire
Studsvik Nuclear
March 1990

TR 90-05

Potential effects of bacteria on radionuclide transport from a Swedish high level nuclear waste repository

Karsten Pedersen
University of Gothenburg, Department of General and Marine Microbiology, Gothenburg
January 1990

TR 90-06

Transport of actinides and Tc through a bentonite backfill containing small quantities of iron, copper or minerals in inert atmosphere

Yngve Albinsson, Birgit Sätmark,
Ingemar Engkvist, W. Johansson
Department of Nuclear Chemistry,
Chalmers University of Technology, Gothenburg
April 1990

TR 90-07

Examination of reaction products on the surface of UO₂ fuel exposed to reactor coolant water during power operation

R. S. Forsyth, T. J. Jonsson, O. Mattsson
Studsvik Nuclear
March 1990

TR 90-08

Radiolytically induced oxidative dissolution of spent nuclear fuel

Lars Werme¹, Patrik Sellin¹, Roy Forsyth²
¹Swedish Nuclear Fuel and waste Management Co (SKB)
²Studsvik Nuclear
May 1990

TR 90-09

Individual radiation doses from unit releases of long lived radionuclides

Ulla Bergström, Sture Nordlinder
Studsvik Nuclear
April 1990

TR 90-10

Outline of regional geology, mineralogy and geochemistry, Poços de Caldas, Minas Gerais, Brazil

H. D. Schorscher¹, M. E. Shea²
¹University of Sao Paulo
²Battelle, Chicago
December 1990

TR 90-11

Mineralogy, petrology and geochemistry of the Poços de Caldas analogue study sites, Minas Gerais, Brazil

I: Osamu Utsumi uranium mine

N. Waber¹, H. D. Schorscher², A. B. MacKenzie³,
T. Peters¹

¹University of Bern

²University of Sao Paulo

³Scottish Universities Research & Reactor Centre (SURRC), Glasgow

December 1990

TR 90-12

Mineralogy, petrology and geochemistry of the Poços de Caldas analogue study sites, Minas Gerais, Brazil

II: Morro do Ferro

N. Waber
University of Bern
December 1990

TR 90-13

Isotopic geochemical characterisation of selected nepheline syenites and phonolites from the Poços de Caldas alkaline complex, Minas Gerais, Brazil

M. E. Shea
Battelle, Chicago
December 1990

TR 90-14

Geomorphological and hydrogeological features of the Poços de Caldas caldera, and the Osamu Utsumi mine and Morro do Ferro analogue study sites, Brazil

D. C. Holmes¹, A. E. Pitty², R. Noy¹
¹British Geological Survey, Keyworth
²INTERRA/ECL, Leicestershire, UK
December 1990

TR 90-15

Chemical and isotopic composition of groundwaters and their seasonal variability at the Osamu Utsumi and Morro do Ferro analogue study sites, Poços de Caldas, Brazil

D. K. Nordstrom¹, J. A. T. Smellie², M. Wolf³
¹US Geological Survey, Menlo Park
²Conterra AB, Uppsala
³Gesellschaft für Strahlen- und Umweltforschung (GSF), Munich
December 1990

TR 90-16

Natural radionuclide and stable element studies of rock samples from the Osamu Utsumi mine and Morro do Ferro analogue study sites, Poços de Caldas, Brazil

A. B. MacKenzie¹, P. Linsalata², N. Miekeley³, J. K. Osmond⁴, D. B. Curtis⁵

¹Scottish Universities Research & Reactor Centre (SURRC), Glasgow

²New York Medical Centre

³Catholic University of Rio de Janeiro (PUC)

⁴Florida State University

⁵Los Alamos National Laboratory

December 1990

TR 90-17

Natural series nuclide and rare earth element geochemistry of waters from the Osamu Utsumi mine and Morro do Ferro analogue study sites, Poços de Caldas, Brazil

N. Miekeley¹, O. Coutinho de Jesus¹, C-L Porto da Silveira¹, P. Linsalata², J. N. Andrews³, J. K. Osmond⁴

¹Catholic University of Rio de Janeiro (PUC)

²New York Medical Centre

³University of Bath

⁴Florida State University

December 1990

TR 90-18

Chemical and physical characterisation of suspended particles and colloids in waters from the Osamu Utsumi mine and Morro do Ferro analogue study sites, Poços de Caldas, Brazil

N. Miekeley¹, O. Coutinho de Jesus¹, C-L Porto da Silveira¹, C. Degueldre²

¹Catholic University of Rio de Janeiro (PUC)

²PSI, Villingen, Switzerland

December 1990

TR 90-19

Microbiological analysis at the Osamu Utsumi mine and Morro do Ferro analogue study sites, Poços de Caldas, Brazil

J. West¹, A. Vialta², I. G. McKinley³

¹British Geological Survey, Keyworth

²Uranio do Brasil, Poços de Caldas

³NAGRA, Baden, Switzerland

December 1990

TR 90-20

Testing of geochemical models in the Poços de Caldas analogue study

J. Bruno¹, J. E. Cross², J. Eikenberg³, I. G. McKinley⁴, D. Read⁵, A. Sandino¹, P. Sellin⁶

¹Royal Institute of Technology (KTH), Stockholm

²AERE, Harwell, UK

³PSI, Villingen, Switzerland

⁴NAGRA, Baden, Switzerland

⁵Atkins, ES, Epsom, UK

⁶Swedish Nuclear and Waste Management Co (SKB), Stockholm

December 1990

TR 90-21

Testing models of redox front migration and geochemistry at the Osamu Utsumi mine and Morro do Ferro analogue sites, Poços de Caldas, Brazil

J. Cross¹, A. Haworth¹, P. C. Lichtner², A. B. MacKenzi³, L. Moreno⁴, I. Neretnieks⁴, D. K. Nordstrom⁵, D. Read⁶, L. Romero⁴, S. M. Sharland¹, C. J. Tweed¹

¹AERE, Harwell, UK

²University of Bern

³Scottish Universities Research & Reactor Centre (SURRC), Glasgow

⁴Royal Institute of Technology (KTH), Stockholm

⁵US Geological Survey, Menlo Park

⁶Atkins ES, Epsom, UK

December 1990

